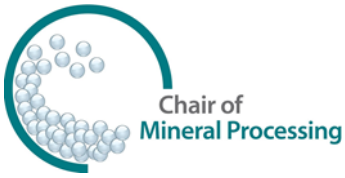

Design, Construction and Performance Test of a Laboratory Column Flotation Apparatus

Conducted at:

Department of Mineral Resources and Petroleum Engineering

Montanuniversität Leoben

Ali Kamali Moaveni

Nov. 2015

Supervisor: Ass.Prof. Dipl.Ing. Dr.mont. Andreas Böhm

Abstract

In order to process material matter of a size smaller than 25 µm by flotation at laboratory scale, an investigation was carried, in order to design a (laboratory) column flotation cell at the Chair of Mineral Processing, which had to be based on the findings of an intense literature study.

The final cell design was manufactured in co-operation with an Austrian provider for construction in plastics. It has an inner diameter of 81.4 mm and 1.83 m tall, having a volume of 9.5 litres. The material which was used as column body is transparent PVC-U to avoid any reaction with chemical compositions. A porous pipe bubble generator, is used to introduce air bubbles into the column.

The instrumentation comprises digital and analog flow meters to measure all liquid flows as well as a differential pressure system to estimate the gas holdup.

In order to evaluate the performance of the apparatus preliminary tests were carried out with feed materials containing naturally hydrophobic talcum and graphite. Samples of the products were analyzed size related for density, LOI, carbon and sulfur content and evaluated by mass balance tables. The results from the single stage tests obtained so far clearly show a separation effect. The LOI content of the talc sample could be decreased from 9 % in the feed to 6 % in the talc concentrate. As graphite experiment, the carbon content is increased from 54.4 % in the feed to 69,2 % in the concentrate. Necessary improvements are discussed.

Keywords: column flotation , physical separation , fine particle processing

Kurzfassung

Auf der Grundlage eines ausgedehnten Literaturstudiums sollte eine Laborflotationssäule entworfen werden, um Flotation im Körnungsbereich unter 25 µm im Labormaßstab betreiben zu können. Die Laborzelle wurde in Zusammenarbeit mit einem österreichischen Unternehmen spezialisiert auf Maschinen- und Apparatebau in Kunststoff umgesetzt. Der Innendurchmesser beträgt 81,4 mm. Die Säule besitzt eine Höhe von 1,83 m und fasst ein Volumen von 9,5 l. Die Instrumentierung umfasst Volumenstrommessgeräte zur Erfassung aller Flüssigkeitsströme und ein Differenzdrucksystem zur Aufnahme der Gasvolumenkonzentration in der Trübe.

Erste Versuche mit Aufgabematerialien, die natürlich hydrophoben Talk und Graphit enthielten, sollten das Trennverhalten darlegen. Proben der Flotationsprodukte wurden korngrößenbezogen hinsichtlich Glühverlust, Stoffdichte, Kohlenstoff und Schwefelgehalt analysiert und im Wege von Bilanztafeln ausgewertet. Die Ergebnisse belegen eindeutig den Trennerfolg. Der Glühverlust im Konzentrat konnte für die Talkflotation von 9 % auf 6% im Konzentrat-Produkt reduziert werden. In den Flotationsversuchen mit graphitreichem Aufgabematerial Kohlenstoffgehalt von 54,4% in der Aufgabe auf 69,2% im Konzentrat gesteigert werden. Notwendige apparative Verbesserungen werden diskutiert.

Keywords: säulenflotation , feinkornaufbereitung , physikalische trenntechnik

ACKNOWLEDGEMENTS

I am indebted especially to Mr. Professor H. Flachberger, head of chair of Mineral Processing at Montan University of Leoben and Mr. Ass. Professor A. Böhm, my supervisor, for them excellent advice, keen, enthusiasm and constant encouragement.

As well, I gratefully acknowledge all my laboratory colleges, Mrs. M. Resch, Mrs. N. Auer, Mrs. A. Balloch and the technical staff Mr. H. Stürzenbacher

I also would like to thank my colleges, DI. W. Lämmerer, J. Strzalkowski, J.A. Gargulak for discussion and help during experiments.

All funding is gratefully acknowledged.

AFFIDAVIT

I declare in lieu of oath, that I wrote this thesis and performed the associated research myself, using only literature cited in this volume.

_____ _____

Date Signature

Content

Objective

Based on the findings of a literature study a laboratory scale flotation cell has to be designed, constructed and implemented into the technicum of the institute of mineral processing.

The column has to be equipped with appropriate measurement systems, in order to characterize all the parameters relevant for the evaluation of the efficiency of the column flotation

The prototype has to be tested with naturally hydrophobic mineral feed material of defined composition, in order to evaluate the functionality of the apparatus. Based on the evaluation of sampling results of the continuous test runs the performance of the device and potential improvements have to be discussed.

Summary

The purpose of this investigation is the design, construction and performance evaluation of a laboratory flotation column. The performance tests serve to identify drawbacks in manipulation and to improve the setup of the flow systems, gas supply and measurement instrumentation where necessary.

The construction is based on the findings of an intense literature study (chapter two). The design was assisted by a free student version of Auto-Cad Inventor software. A commercial tube bubble generator was selected. The inner diameter of the cell body, having 81,4 mm, is adjusted to the characteristics and dimensions of the generator. Also, the dewatering capacity at the laboratory of the chair of mineral processing is taken into account in the current capacity considerations.

The column is built of different modules, each of which easy to access, that can easily be assembled and disassembled in case of unforeseen problem. The height of the cell mainly influences the retention time, thus the obtainable grade and the recovery. In order to adapt the column to the flotation characteristics of different materials the height of the cell can easily be changed. For the current applications a height of 1,82 m is selected. Based on the literature, the feed port is placed at two third of total column height from the cell bottom. The column is designed to perform at semi-batch condition. A conditioning tank with a capacity of 50 litres was applied to prepare the feed suspension for the flotation process. The minimum necessary conditioning tank volume to achieve stable conditions, should be three or four times more than the reactor volume, according to literature. The capacity of conditioning tank was selected five times bigger than the cell capacity (9,5 litres)

The column was manufactured in cooperation with an Austrian provider for construction in plastics. PVC-U is selected as the material for the cell, because of its chemical stability and transparency.

The conditioning tank was equipped with a high speed impeller for pulp conditioning at the desired solid content and reagents dosage. A digital flowmeter was also applied for feed flowrate determination.

Talc and graphite ores were chosen as experimental material to check the performance of the constructed cell due to the following reasons:

- The material is easy available and can easily be prepared for the flotation experiments in the amount of needed.
- The mineralogy and physical properties are known
- Simple reagent system, due to the natural hydrophobicity of the valuable minerals apply.
- No chemical impact on waste water and filter cake due to reagents.
- Flotation efficiency can be evaluated by physical analysis of LOI and density measurement.

The particle size distribution as well as the characteristics of the used samples, for both talc and graphite ore types, are given in chapter five.

The talc feed sample was ground to a 100% -50 μm by the vertical roller mill of the institute of mineral processing in open circuit, making use of selective breakage behaviour of talc. LOI and density measurements in the size fractions +25 μm and -25 μm prepared from sample of the feed and the flotation products served to trace the performance of the cell in the coarse and fine size range. The experiments were carried out in continues mode.

The detailed flotation conditions on talc ore are given in chapter five. The solid concentration of feed pulp was adjusted at 4%. Based on the obtained results, a fluctuation was observed in the LOI of the concentrate and LOI recovery against time duration of flotation. From the back calculation of feed characteristics, the third series of sampling is in best agreement with the nominal feed properties and thus shown in table 1.

Table 1: The third sampling results of talc ore column flotation

Stream	Yield (%)	Fraction (μm)	Mass (%)	LOI (%)	100-LOI (%)	Recovery	
						LOI (%)	100-LOI (%)
Concentrate	34,3	+25	50,62	5,24	94,76	21,5	35,7
		-25	49,38	6,79	93,21		
SUM			100,00	6,01	93,99		
Tailing	65,7	+25	21,18	9,65	90,35	78,5	64,3
		-25	78,82	11,94	88,06		
SUM			100,00	11,45	88,55		
Feed	100	+25	31,29	7,20	92,80	100,0	100,0
		-25	68,71	10,67	89,33		
SUM			100,00	9,58	90,42		

A single stage rougher flotation test, in batch mode, was committed with the mechanical laboratory flotation apparatus (type Denver) using the 1,6 litres cell delivered at equal conditions with regard to reagent dosage and solid concentration. The results of the test are given in table 2.

Table 2: the results of the mechanical flotation test

Stream	Yield (%)	Fraction (μm)	Mass (%)	LOI (%)	100- LOI (%)	Recovery (%)	
						LOI	100- LOI
Conc.	60,2	25	20,8	5,2	94,8	40,8	62,1
		-25	79,2	6,4	93,6		
SUM			100,0	6,2	93,8		
Tail	39,8	25	18,6	9,2	90,8	59,2	37,9
		-25	81,4	14,5	85,5		
SUM			100,0	13,5	86,5		
Feed	100,0	25	19,9	6,7	93,3	100,0	100,0
		-25	80,1	9,7	90,3		
SUM			100,0	9,1	90,9		

The performed tests with graphite ore are described in detail in chapter five. At 2% solid concertation of feed pulp, the carbon grade could be increased from 54,4% in the feed to 69,2% in the concentrate at a concentrate mass recovery of 61%. At 4% feed pulp solid content, the carbon grade could

be increased from 54,4% in the feed to 68,6% in the concentrate at a concentrate yield of 45,3%

Fluctuations in the result of column flotation tests on talc and graphite ore should give reason to the following improvements in the future;

- Application of pumps for feed and underflow streams for stabilization of the flotation operation conditions.
- Investigation on wash water flowrate and optimum bias rate
- Investigation on air volume consumption and gas holdup measurement
- Simulation of flotation rate against duration of flotation
- Investigation of minimum flotation duration to achieve stable conditions

Chapter One:

Flotation Machinery

1-1- Introduction

Basically, the flotation process is implemented by means of differences in surface chemistry properties of the particles (hydrophobicity of the particle species). It is a highly versatile method for physically separation of particles. The froth flotation process is used in many industrial cases for separation such as waste paper deinking for paper recycling, mineral separation and coal preparation to separate the valuable minerals from the non-valuable material.

The Potter process was introduced to flotation in minerals industry in 1905. The first major commercial application of froth flotation was the production of sphalerite concentrate in Australia [1]. Following that initial, the application of flotation process was spread quickly all over the world and remained as an essential process in mineral beneficiation.

A simple explanation of flotation is, that it is not energetically favourable for hydrophobic particles to residue wholly within the liquid. Given the chance, the hydrophobic particles will attach to the air bubbles whereas the hydrophilic particles would not attach to the air bubbles and fall in the column to the unfloated material discharge. Nowadays, the flotation column has became very popular in different areas of industrial mineral beneficiation [2]. Less entrapment of gangue particles in the floated fraction, especially for fine particle processing, lower energy consumption, higher capacity related to the needed land field and lower capital requirement are the most important advantages in industrial processing plants [2].

Even though the flotation column is capable of producing better grades than the conventional mechanical cells, this machine is an industrial reactor that has not been yet fully understood. The superiority of the column is attributed principally to the bubbling regime and to the presence of a depth cleaning zone (froth) [3].

Flotation columns work on the same basic principle as mechanical flotation equipment – mineral separation takes place in an agitated and/or aerated water mineral slurry, where the surfaces of the selected minerals are made water-repellent by conditioning with selective reagents. The particles which attached to the air bubble are floating on the surface of the cell while

wetted particles stay in the suspension phase and discharge from the bottom of the cell. However, there is no mechanical mechanism causing agitation and separation takes place in a vessel of high aspect ratio. Air is introduced into the cell through spargers creating a countercurrent flow of air bubbles. This type of flotation cells, column flotation, offers many advantages including [3]:

- Metallurgical performance improvement
- Possibility of beneficiation of fine and coarse particles
- High selectivity
- Simple process control
- Effective process of heavy loaded slurries
- Absence of moving parts
- Less energy consumption
- Lower capital requirement
- Less required land field

Increase in the size of single flotation units was the main development in the evolution of flotation machinery. For instance, the large machines in 1950 were of 1,35 m^3 capacity while, in 1989, the volume of large machine is 85 m^3. These advances lead mining industry to process ores of lower grade due to lower operating costs [4].

The flotation process has been invented in the early 1900´s. In general, flotation machines are categorized into two types; mechanical and pneumatic machines [4].

1-2- Mechanical Machines

Mechanical flotation devices are most widely used in the mineral processing industry. In this type of machines, the turbulence of flotation environment is provided via mechanical parts such as impeller, motor and a clutch.

In the mid 1960s, the largest flotation machine offered by Denver was 2,8 m^3, by Wemco 1,7 m^3 and by Galigher 1,1 m^3 volume. The Denver 2,8 m^3 cells were installed as a satisfactory machinery due to their reasonable

price. At this time, high capacity processing units became more popular, because of decreasing of ore grades. High capacity of operation is an important factor to process low grade ores economically [4].

Denver, Galigher and Wemco are developed to 340 m^3, 42,5 m^3 and 85 m^3 cells, respectively.

1-2-1- Mechanical machines set up

There are many design parameters influenced. The first design parameter is tank geometry. The geometry of the cell can be square, rectangular, circle or U- shaped. Another effective parameter in flotation machine design is the impeller geometry. The major differences are include size, shape and the number of rotor and stator blades. The design of the rotor and stator has a deep influence on the power consumption of the device. The ratio of flow to shear is also determined by the impeller rotational speed. This parameter is a function of rotational speed and diameter of impeller. This ratio is decreasing when the cell becomes larger, which is an advantage. In the case, the baffles are not designed properly, high agitation disrupts the froth. In addition throughput, which is defined as the mass of dry solid in a defined time per cubic meter of the cell volume, has a deep effect on the machinery design. The higher throughput at constant power consumption refers to the lower specific power. One of the most important advantages of larger flotation cells is the substantial reduction of specific power requirement [4].

1-2-2- Cell types

Galigher subsequently developed a flotation machine with 6 m^3 volume, however they offered originally 1,1 m^3 cells. Nowadays, the Galigher Agitair machine is not in the market any more.

WEMCO is one of the largest suppliers of flotation machines and manufacturer of Agitair. The impeller is a multibladed rotor with a cylindrical stator.

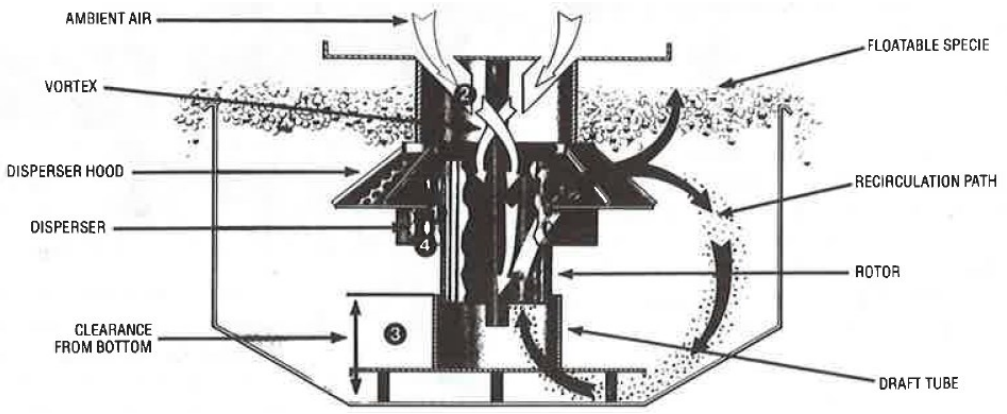

Fig. 1-1: WEMCO Flotation Machine [4]

The OK mechanism and U-shaped tank are the two features of the Outokumpu "OK" flotation machine. The U-shaped tube is used to provide better suspension and air dispersion leading to lower power consumption. As it has been shown in fig. 1-2, the impeller has vertical blades, narrower at the bottom and separate slots for air and slurry [4].

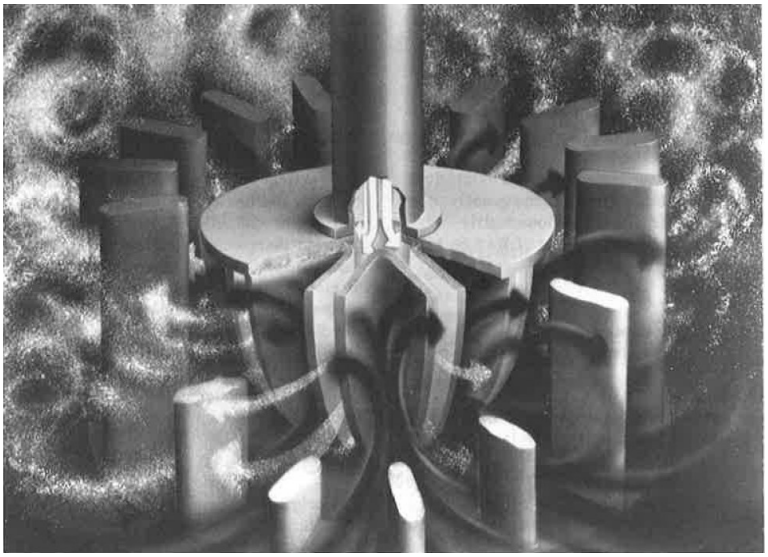

Fig 1-2: "OK" Outokumpu Flotation Mechanism [4]

The original design of Denver is a cell-to-cell machine. In this generation of cells, air is self-induced, drawn in from the atmosphere through the impeller system.

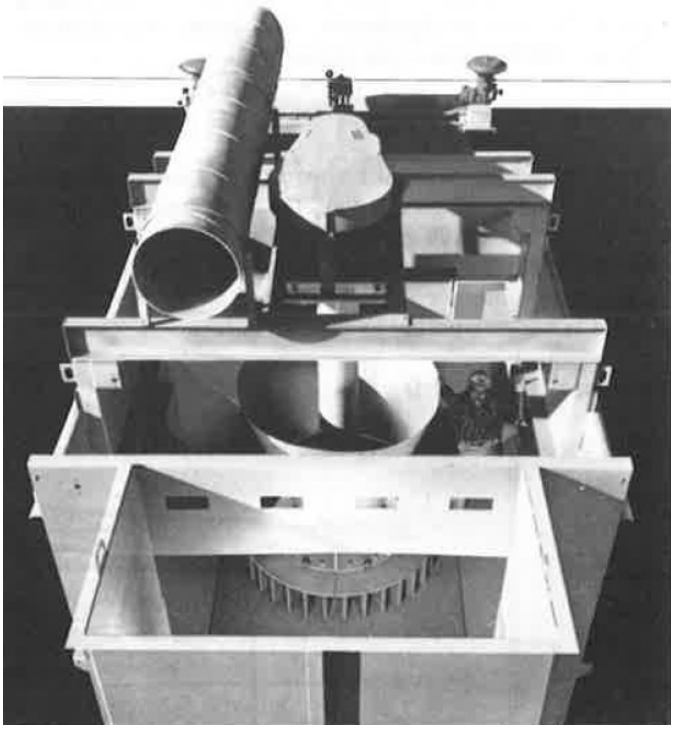

Fig. 1-3: Denver D-R Machine [4]

The aim of Sala was to minimize vertical circulation. Usually, the impeller is large in diameter compare to the tank size to avoid solid settling.

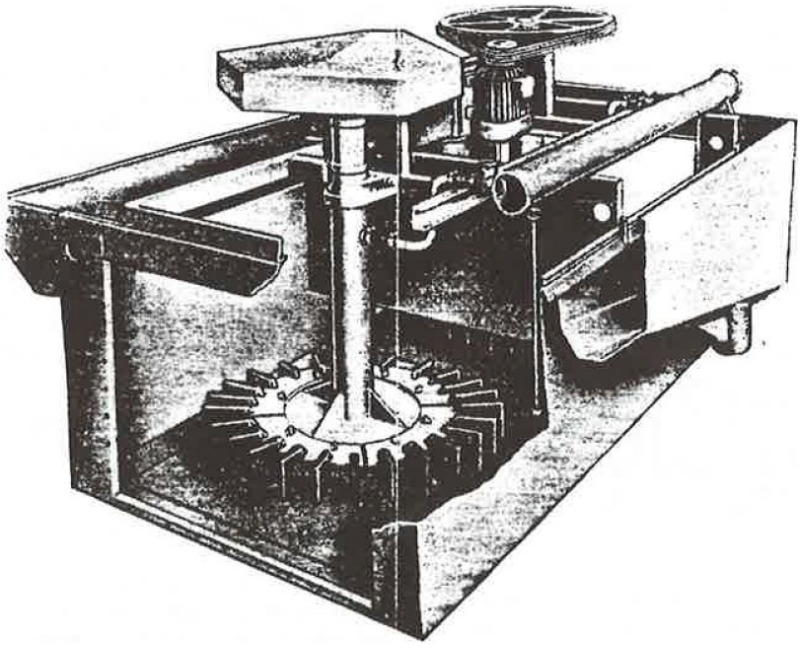

Fig. 1-4: Cut-away view of Sala Flotation Machine [4]

In the Maxwell cell type, agitation is provided by a radial flow turbine impeller, which is connected by a sparger directly to the impeller. Some of the advantages of Maxwell are; low rate of air usage, capital cost and specific power draw.

1-3- Pneumatic machines

1-3-1- Pneumatic cells

In pneumatic machines, the agitation is carried out, in absence of mechanical parts and impeller, by an aeration system in the slurry, that leads to lower maintenance costs. The pneumatic machines are no longer in use. The volume capacity of this cell is high for easy floatable material compared to the other types of machines. Therefore, the power consumption of this type of flotation machine is low per ton of ore processed [4].

1-3-2- Column Flotation

The second group of pneumatic flotation machine is column flotation. This type of flotation cell was developed by Boutine in 1960, was an alteration from conventional flotation cells. Some of the advantages are; lower energy consumption, lower area for installation, higher capacity and lower operation costs.

Typically, there is a deep foam layer in a flotation column, whereas conventional flotation machines usually support very little foam indeed. Fig. 1-5 & 1-6 illustrates a schematic representation of a column flotation cell.

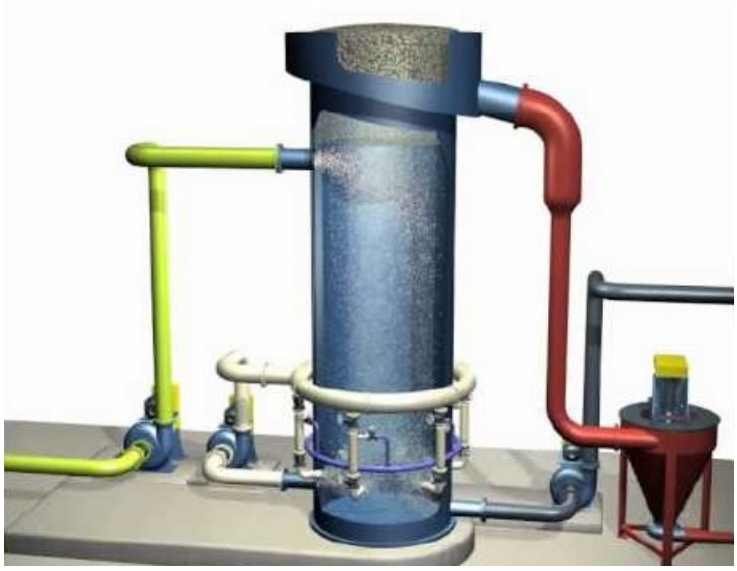

Fig. 1-5: Industrial Metso Flotation Column [5]

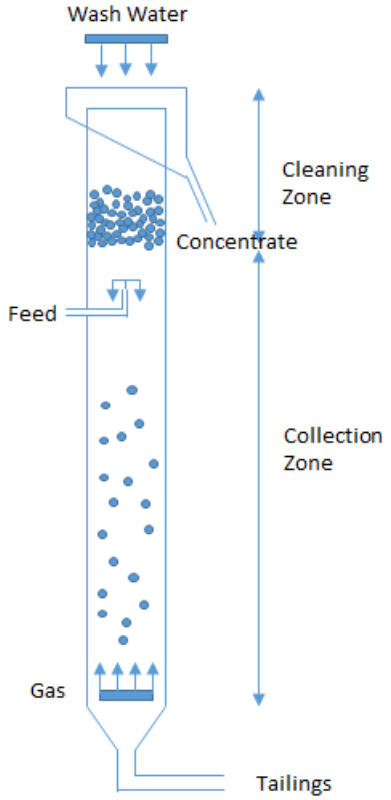

Fig. 1-6: A schematic diagram of column flotation cell [6]

In figure 1-6, in the collection zone, the hydrophobic particles have the opportunity to attach to the bubbles and are transported up the column

into the foam layer, which is known as the cleaning zone. The hydrophilic particles, which are not supposed to attach to the bubbles, but are entrapped between the hydrophobic particles would wash in the cleaning zone via wash water and rejected into the suspension [6].

Column flotation was invented by Boutine in 1960. Flotation column cells are used in various applications. However, the main purpose of the column cell is improvement of final concentrate grade to a level that would not be possible using conventional flotation [6]. In many cases, the use of column flotation enables a concentrate to achieve separation that is closer to perfect than any other type of froth flotation device.

The true advantage of column comes in the form of profitability. Columns allow mineral beneficiation plants to achieve higher profits of their concentrate by purifying concentrate, lower shipping costs, decreasing plant foot print and lower smelter penalties. Low operating and maintenance costs due to the absence of mechanical moving parts are another advantages of the flotation column [7].

The flotation systems includes many interrelated components. Changes in one area will produce compensation effects in other areas.

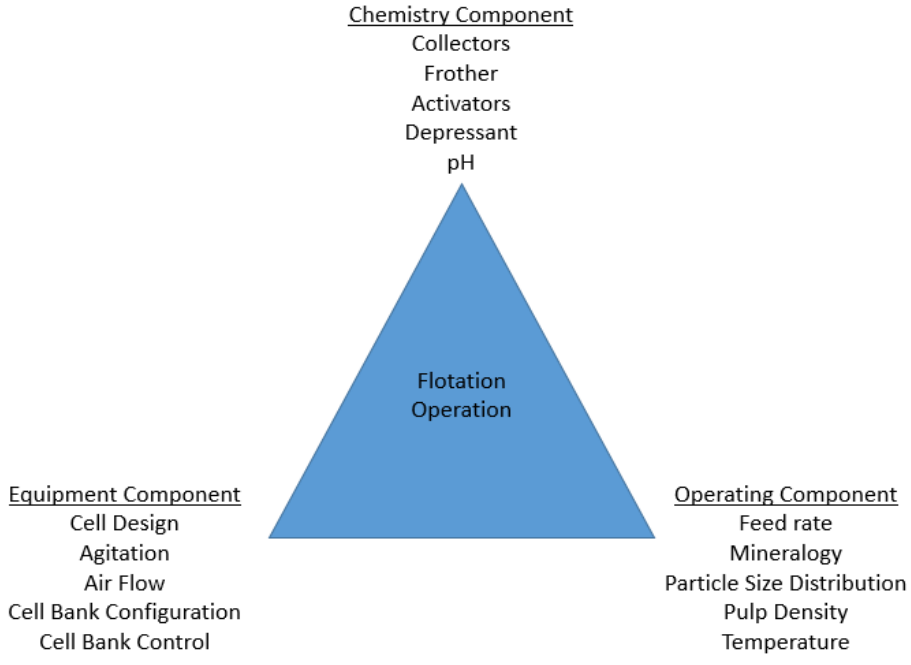

Fig. 1-7: The interrelated components with flotation system [7]

It is therefore important to take all of these factors into account in froth flotation operations. Changes in the settings of one factor will automatically cause or demand changes in other parts of the system. As a result, it is difficult to study the effect of any single factor without consideration of interaction effect.

Chapter Two:

Flotation Column

Many parameters are of influence on the column flotation performance. Some of them are common in all types of flotation devices, but some others are introduces just for column cells due to special properties of flotation column reactors [8].

2-1- Effective parameters on the column performance

2-1-1- Types of apparatus

There are mono-cells and multi sectional apparatus. The latter being sub-divided into two groups; column with co-current of slurry and air flows, and apparatus combining co- and counter current sections.

The movement characteristics of particles and air bubble are the major factor concerning the probability of flotation aggregate formation, coverage degree of bubble surface, power requirements and flotation rate of the process. The counter current regime provides better conditions for enhanced aggregate stability and particle- bubble attachment. The probability of particle- bubble collision and particle attachment is determined in particular by the normal component of their inertia forces, contact time and relative velocity. Relative particles and bubble velocity in a counter current at a slurry flow rate of 2 cm/s and a mean bubble size of 1,5- 2,5 mm is about 10-12 cm/s [7]. The relative particle and bubble velocity corresponds to optimum collision condition work. The rise velocity of the swarm of bubbles, in a counter current of slurry and air flow is reduced. This increases their retention time and rises the coefficient of air utilization and specific throughput of the apparatus. The inertia forces that might break down the particle bubble aggregate are insignificant in a flotation column. In an upward slurry flow particles retention time is given by Eq. 1 [8];

$$\frac{2U_p}{U_l - U_p} \qquad (1)$$

Where:

U_p … $Particle\ sedimentation$

U_l …. $Liquid\ flow\ rate$

Eq. 1 is more significant for coarse and low floatability particles.

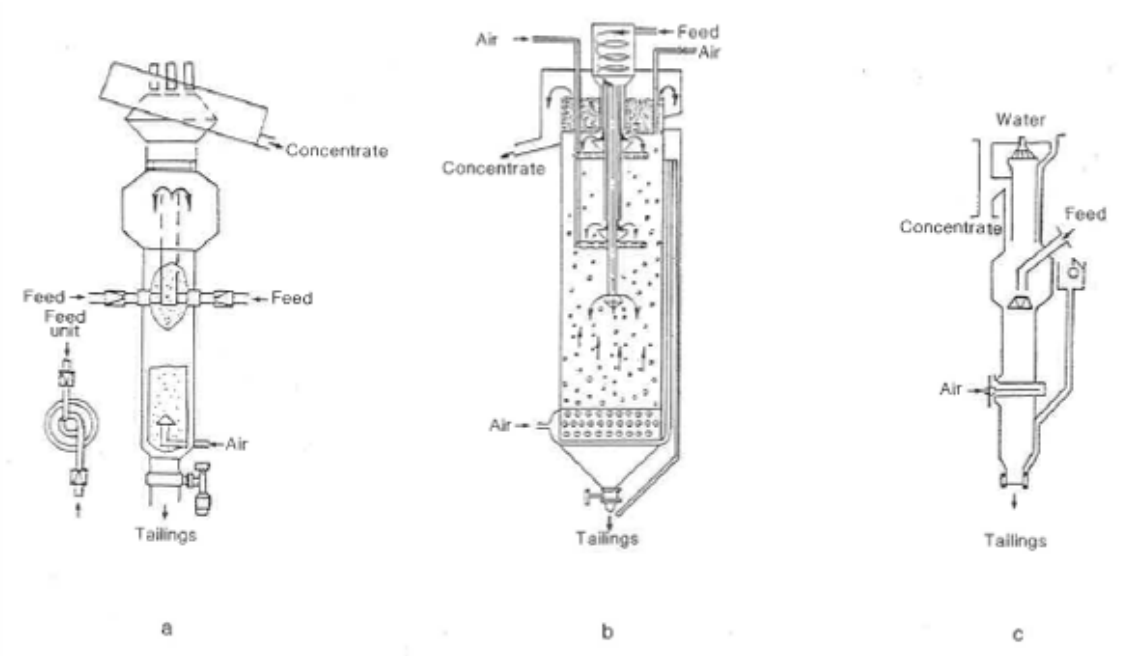

Fig. 2-1: Flotation Column developed in Gintsvetmet, a) IMR, b) Gosgorchipproject, c) Institutes [8]

2-1-2 Wash Water

Wash water usage is a special property, implemented on column cells. The main task of wash water is washing entrapped hydrophilic particles back into the collection zone. Entrapment phenomena is one of the main reasons for concentrate contamination during attachment mechanism [3]. The wash water stream must be large enough to penetrate the top layer of the froth, because the washing action takes place primarily at the froth-pulp interface [9]. If the water stream is too light, there will be a tendency for the water to bypass the froth directly into the over flow. Heavy wash water flowrate can also destroy loaded bubble and reduce recovery significantly. In some cases, for heavy froths, it is also possible to install the wash water pipes below the top of the froth.

Therefore, both wash water flowrate and nozzle positioning are counted as effective parameters on the grade and recovery of overflow stream [3].

2-1-3- Bias

The difference between wash water flowrate and concentrate water flowrate is referred to as the bias. If the wash water flow exceeds concentrate water flow, the bias would be positive and the bias would be negative when reverse occurs. A common approach with column flotation is to operate the process wih a bias range of zero. Bias can be expressed as a superficial velocity (J_B cm/s) [3].

2-1-4- Required Bias Flow

According to the Fig. 2-2, as operating bias is decreased, the carrying capacity will increase. Decreasing the wash water rate or increasing the gas rate can also decrease the bias rate [3]. The example of the latter is indicated in Fig. 2-3. The results of the bias and gas rate were obtained from the rougher column flotation on copper ore with 10 cm diameter of the column cell. The data in fig. 2-3 was derived with two sparger fabrics, with fabric 2 being considerably more permeable than fabric 1 and thereby generating larger gas bubble than fabric 1. The generation of larger gas bubbles can be inferred from gas holdup measurement.

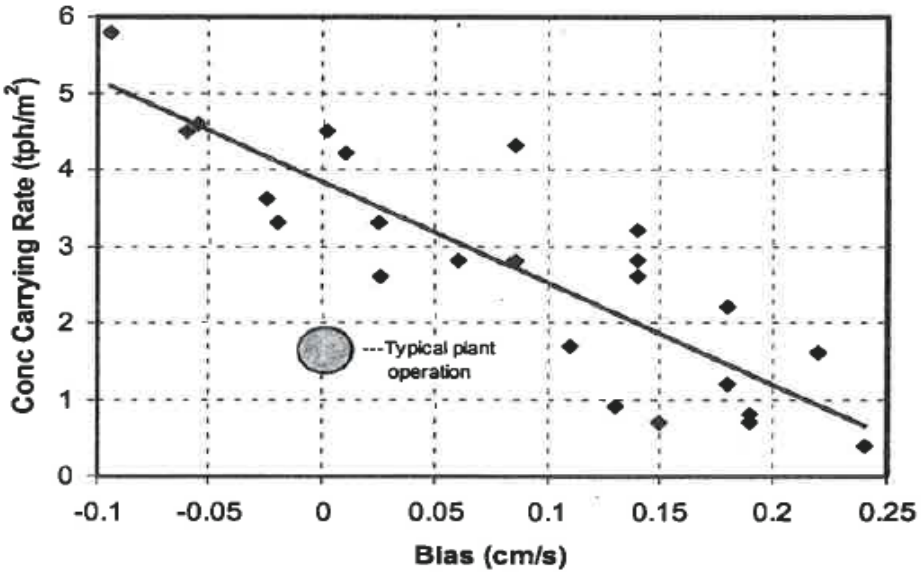

Fig. 2-2: Concentrate solid carrying rate versus bias rate [3]

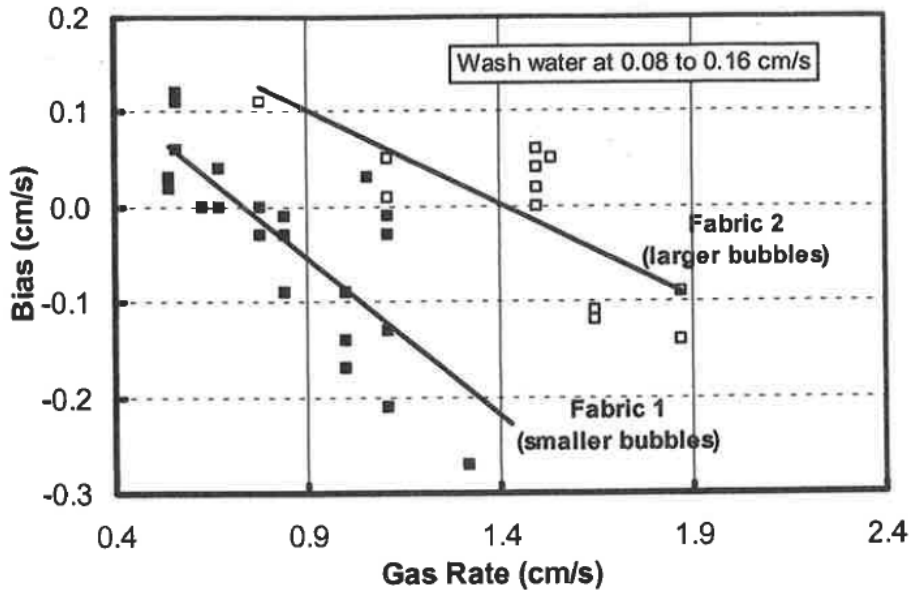

Fig. 2-3: Effect of gas rate and bubble size on bias [3]

It has been demonstrated that operation of a column at zero to slightly positive bias will usually maximize the concentrate grade [10&11]. More increase in bias to significantly above zero bias will result in minimal grade increase but a substantial recovery loss. An example is shown in Fig. 2-4 by using a column of 10 cm diameter.

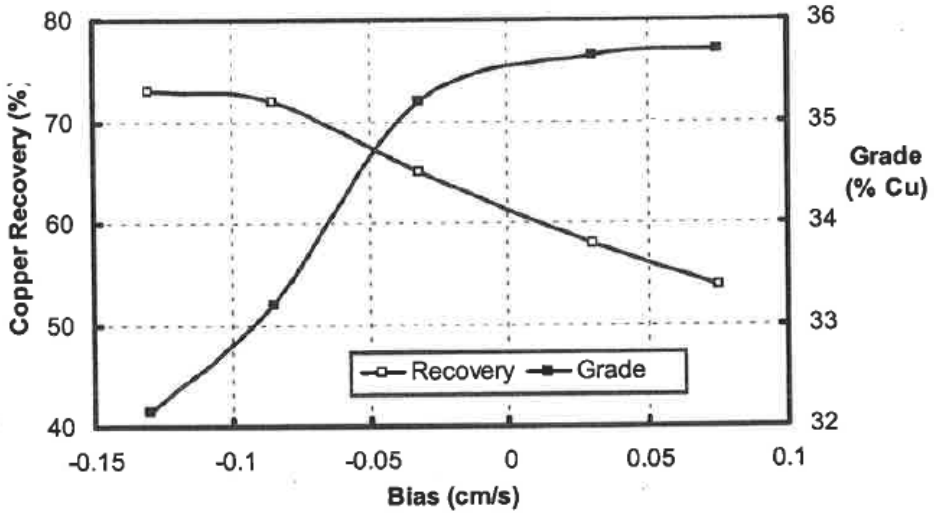

Fig. 2-4: Effect of bias on grade and recovery [3]

In some cases, it would be more profitable to run with a slightly negative bias. A situation like this, arises when the column must process high grade feed. If insufficient column capacity has been installed, it will be difficult to operate the column with a positive bias while still attaining target recovery.

The study, which has been carried out at Laval University demonstrated the feasibility of an independent sensor for bias, which models the relation between the conductivity profile across the interface and the bias value using a neural network algorithm. A 250 cm height, 5.25 m diameter plexiglas laboratory column was equipped with a series of conductivity electrodes in its uppermost part (across the interface) to measure both, the interface position and the bias rate. Using such equipment, the flotation column dynamics was identified [12].

2-1-5- Gas Holdup

The gas holdup is the content of air inside the column. It is one of the most important parameters since it characterizes the hydrodynamics of bubbles in the co1umn cell [23, 24] and is a determining factor of the quantity of bubble surface available for particle attachment. The gas holdup is a function of a variety of variables in flotation and dependent to the bubble size, which is a function of sparger type, frother properties, air flowrate, compressed air pressure, machine and operational conditions, chemistry, pulp flowrate, solid content and pattern of mixing in the collection zone. Gas holdup is related to the flotation kinetics and defines the bubble surface area flux. [13]

When gas is introduced into a column cell, liquid or slurry is displaced. The volumetric fraction displaced is called the gas holdup (ε_g) [13]. The gas holdup is the fraction of gas in a gas-liquid or gas-pulp mixture. The complement is the liquid or slurry holdup (1-ε_g). The gas holdup is a function of both gas rate and bubble size [3]. The magnitude of gas holdup is a clue to the hydrodynamic condition of the collection zone.

The column feed port divides the column into two different zones. In case that the lower zone contains 10% to 30% air, it is deemed to be responsible for the bubble-particle attachment (i.e. for mineral recovery), whereas the upper zone, which exhibits a 70 to 90% gas hold-up, is responsible for the concentrate cleaning. This difference in gas hold-up allows the detection of the interface between both zones, either by visual observation in a transparent column or through any property related to the air content, such as electrical conductivity, pressure or specific gravity [12]. The interface position, also called pulp level or froth depth, is another important parameter of the column operation since it determines the relative height of both zones. A taller bottom zone provides more residence time for the bubbles to collect the mineral particles, thus increasing the recovery. Consequently, this zone is called the collection zone or recovery zone [12].

The superficial velocity can be calculated by dividing the flowrate by the column cross-sectional area. Hence, gas flowrate is often expressed as a gas velocity J_g (cm/s). The range of J_g observed in industrial flotation columns, at the top of the column, is typically between 1-2 cm/s [12].

$$J_g = \frac{Q_g}{A} \qquad (2)$$

Where:

J_g ..... Superficial gas rate (cm/s)

Q_g .... Volumetric flow rate of gas (cm^3/s)

A ..... Cross-sectional area (cm^2)

2-1-6- Gas holdup measurement

The techniques for the measurement of gas holdup can be classified into two categories: local and global measurements. Each of these methods are described as follow.

a) Local Methods

Of the local measurement techniques, the most frequently used methods are based on either electrical conductivity or X-ray absorption which depends on the concentration of each phase [14]. In industry, because of a lack of reliable method for on-line gas holdup measurement, it has been considered as an unmeasured variable untill 2001. By this time a new conductivity probe was developed to measure the electrical conductivity of the slurry-gas dispersion [13].

Measurements have been performed in a 50 cm diameter and 4 m length laboratory column flotation cell. In this column air is introduced by eight vertical cloth spargers in a 40 cm ring through the column as shown in fig. 2-5. The probe has been calibrated with some measurements which are carried out by filling the cell completely with pure water. The actual gas holdup values are determined during the experiments according to the standard method, by means of pressure difference between two defined points as will describe later. These series of experiments are carried out at several air flowrates, using pure water, with and without surfactants [13].

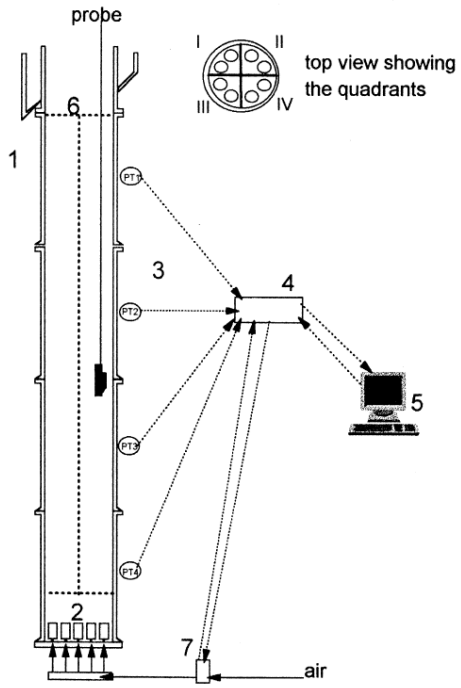

Fig. 2-5:(1) Flotation Column, (2) Spargers, (3) Pressure Transmitters, (4) Serial Communication Interface, (5) Computer, (6) Vertical Baffles, (7) Mass flow Controller [13]

As a result of the measurements, the gas holdup value obtained from conductivity is compered well with those from pressure difference in fig. 2-6.

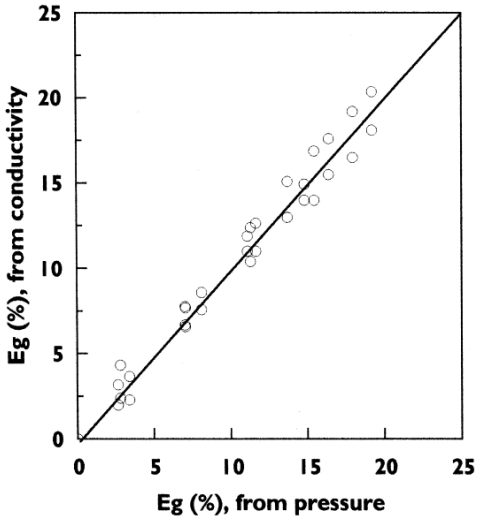

Fig. 2-6: Experimental result in two-phase water/air system [13].

The gas hold up value is also checked horizontally at different positions. Following positions were chosen at the main vertical axis of the column, midway between centre and body of the cell and the wall of the cell via conductivity probe. The results illustrated that the gas holdup is decreasing during its movement from vertical centre axis of the cell to the cell body [13].

b) Global methods

There are two global methods, bed expansion and the manometric technique based on pressure drop along the column. In a study, using the cell shown schematically in fig. 2-7, global measurements were used. Each measurement of gas holdup was repeated at least three times and the average result is presented in all the following figures [14].

Fig. 2-7 shows the laboratory column set-up which is used for gas holdup measurement. The column was constructed using a Plexiglas tube. For most of the tests, water was the only feed and was fed through the wash water inlet. Water flow rate was controlled by a variable speed pump (Masterflex), and the discharge flowrate was controlled by a “Moyno” pump.

Compressed air was introduced into the column through a variety of spargers whereas a flowmeter, calibrated at 20 psi, was used to regulate gas flow [14].

It was found that when no froth zone exists at the top of the column, the two global methods are in good agreement. All experiments were performed at room temperature.

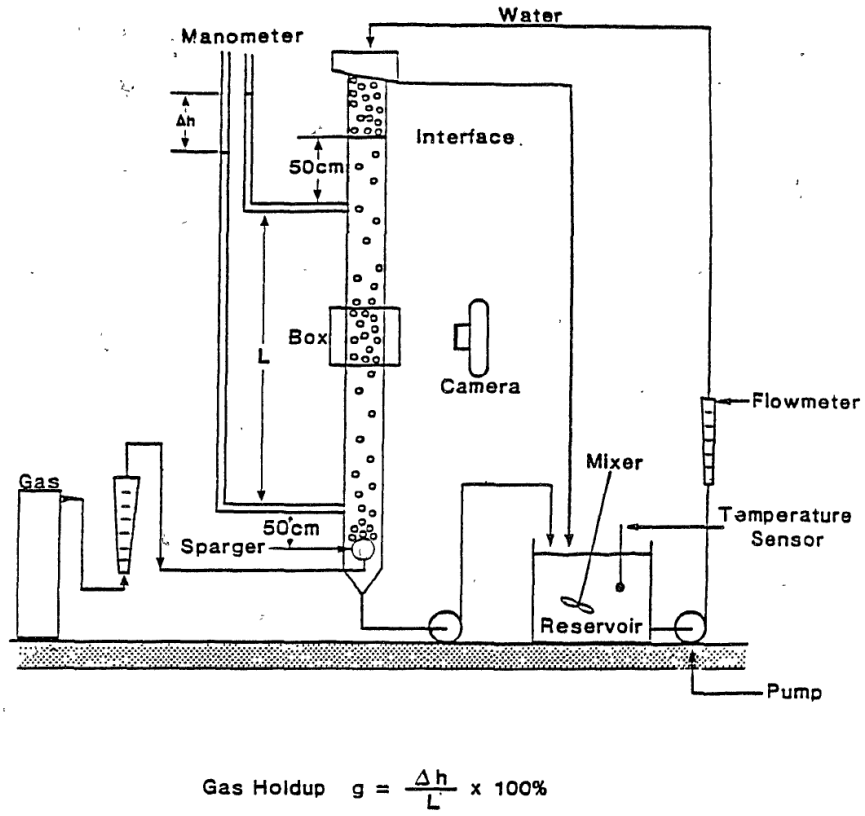

Fig. 2-7: Laboratory Experimental Set-up [14]

The relationship between ε_g and J_g is used to define the flow regime [18]. Fig. 2-8 shows the general relationship between superficial gas velocity and gas holdup. Gas holdup increases approximately linearly, then deviates above a certain range of J_g [15].

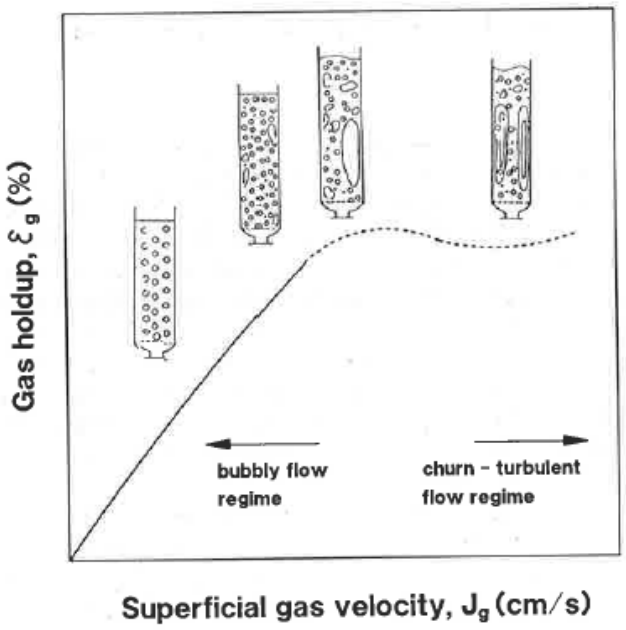

Fig. 2-8: Gas holdup as function of gas rate [16]

2-1-7- Bubble Generation

Bubble generation in column flotation cells is achieved via sparging through pierced rubber or woven fabric such as USBM (US Bureau of Mines) / Cominco and Minnovex. Some disadvantages of these sparger types are:

- Blockage
- Tearing
- Need to shut down to change
- The large number required to maintain bubble size below 2-3 mm.

That approach is not common anymore, because of assessment or replacement problems.

The second sparger types are those which are developed by the means of jetting and shearing like Microcel^{TM} Column and the pneumatic cell [14,15&17].

In jetting techniques, bubbles form as a result of instabilities on the jet surface. Air is forced under high pressure (30-100 psig) and creates a jet of

air through the slurry. The bubble diameter is affected by the jet velocity. This means a higher jet velocity produces smaller bubbles [16 & 17].

$\rho_J v_J$..... jet momentum (per unit volume)

$n_B \propto l_J$

$d_B \propto \frac{1}{l_J}$

$l_J \propto \rho_J v_J$

n_B ..... the number of bubble

d_B ..... bubble size

l_J..... jet length

As illustrated above, for producing a large population of fine particles, a long jet length is required. Jet momentum can be increased by increasing either the density or the velocity. In the USBM and Cominco design, ρ_J is increased by a small addition of water to the gas (normally ~ 1% of the gas volume [14].

With the Minnovex, the approach is to control v_J by adjusting the annulus dimension and the gas pressure. A small annulus width (~1mm) and gas pressure above ~45 psig together result in a velocity between 200- 400 m/s and produces at least a 50 cm long jet [17].

In Microcel™ column sparger, shear is achieved by the force slurry and air over the blades of an in-line static mixer [18]. In the pneumatic cell, feed slurry is forced through a constricted opening, reaching velocities of ~ 4-6 m/s. with this setup, bubbles are produced by introducing air at a right angle through a slot into the column. Due to the slurry velocity, the air is sheared into fine bubbles.

2-1-8- Sparger Types

(a) Steel Sparger

The stainless steel sparger is available through the Flotation Column Co. of Canada Limited. The number of orifices per unit area (porosity) is quite low with respect to the dead area. The enlargement indicates, the holes are not circular and there is a distribution of hole sizes. The average diameter is approximately 50 µm. In addition, the orifices are distributed randomly and the number of holes per unit area is difficult to estimate [14].

(b) Rubber Sparger

This type of sparger was recommended by Wheeler [19] and used at Mines Gaspe. A photograph of the texture shows the regular distribution of holes. The estimated porosity is around 42% and the average orifice diameter is around 80 µm.

(c) Ceramic Sparger

The ceramic sparger was obtained from Fisher Scientific Inc. and is often used in laboratory columns [86]. The average orifice diameter is 60 µm. The photography shows that the distribution of orifices is random and porosity is higher in comparison with steel and rubber spargers. The texture image indicates the shape of the orifices is not circular.

(d) Filter Cloth Sparger

Filter cloth sparger is a commonly used in "home-made" columns, due to its low price and being easy to build. The structure is completely different compared to the other types of sparger. It is not possible to estimate holes size [14].

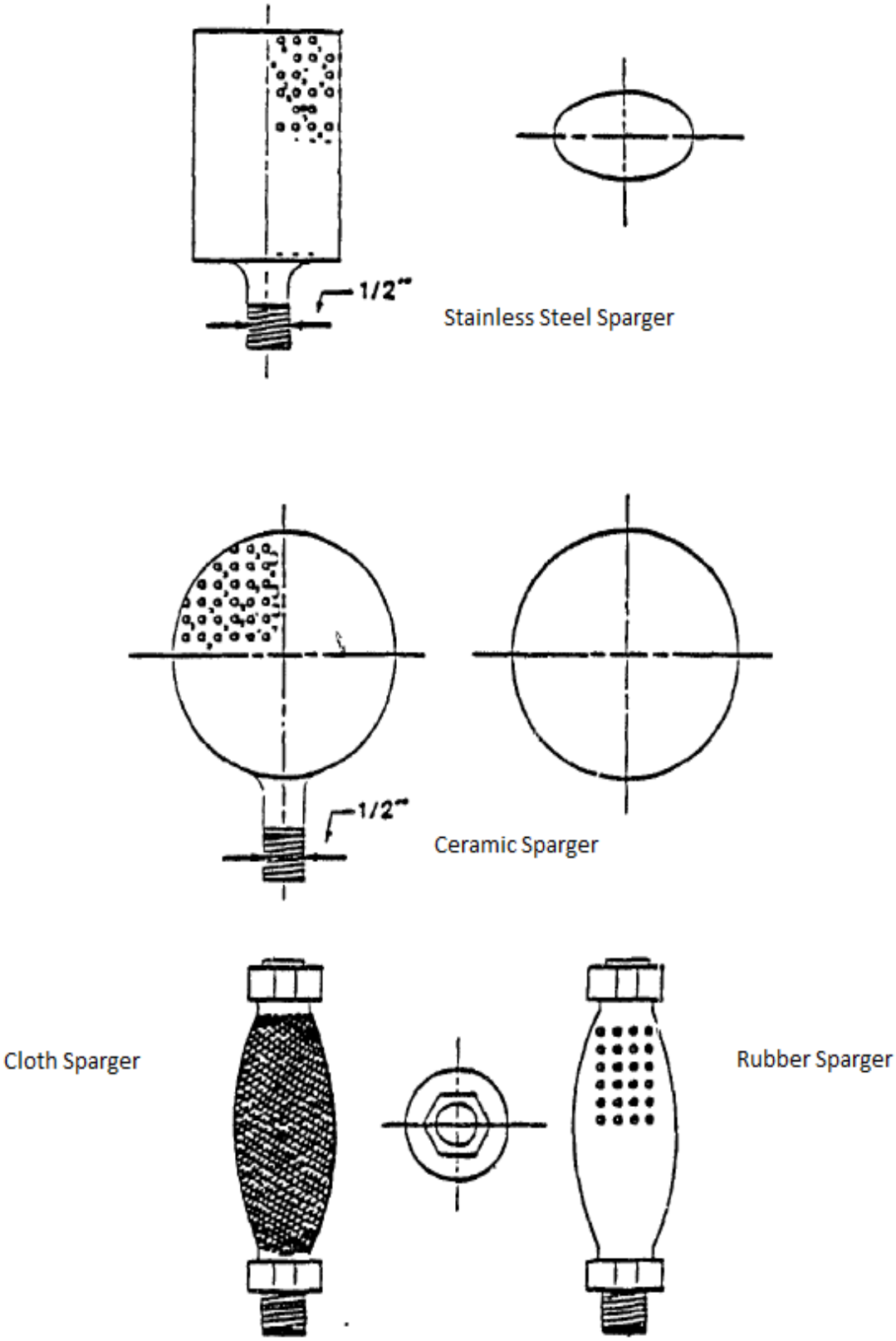

Fig. 2-9: Different types of spargers [14]

Table 2-1: Important properties of sparger types [14]

Type	Orifice dia. (µm)	Surface area (cm²)	Porosity (1/cm²)
Steel	50	20-60	10
Rubber	80	56	42
Cloth	--	37,8-213,63	--
Ceramic	60	19-57	140

2-1-9- Bubb1e Size Estimation

Several methods for measuring bubble size have been proposed. The most frequently used is photography either used directly or to calibrate a proposed alternative method [14&8].

Photography is tedious and restricted to vessels with transparent walls and relatively low bubble concentrations. Thus, for flotation column, it is either used to detect bubble size directly.

2-1-10- Dobby's Method

This method uses the concept of drift-flux to relate phase flow rates and gas holdup to physical properties of a two-phase system. The slip velocity (U_s) is the velocity of one phase relative to another. In Eq. 3 (+/-) refers to countercurrent and concurrent flow, respectively. For counter-current flow of gas bubbles and water in a bubble column the relative velocity U_s is [14]:

$$U_s = \frac{J_g}{\varepsilon_g} \pm \frac{J_{sl}}{1-\varepsilon_g} \qquad (3)$$

Where:

J_g ..... Superficial gas velocity (cm/s)

J_{sl} ..... Superficial slurry or liquid velocity (cm/s)

ε_g ..... Fractional gas holdup (%)

A ..... Machine cross-sectional area (cm²)

The bubble surface area flux is derived as;

$$S_b = 6 * {J_g}/{d_b} \qquad (4)$$

Wallis [20] also postulated that Us is a function of terminal rise velocity U_T of a single bubble and the gas holdup, in the following form:

$$U_s = U_T(1 - \varepsilon_g)^{m-1} \qquad (5)$$

Where, "m" is a parameter defined according to Richardson and Zaki [21] for 1<Re<200

$$m = \left[4{,}45 + 18\frac{d_b}{d_c}\right] * Re^{-0{,}1} \qquad (6)$$

And for 200<Re<500

$$m = 4{,}45 * Re^{-0{,}1} \qquad (7)$$

And the Reynold number is defined by:

$$Re = \frac{d_b U_T \rho_L}{\mu} \qquad (8)$$

Where;

U_T ..... Terminal rise velocity of a single bubble (cm/s)

U_T is calculated by Eq. 3 and assuming ε_g=0

Combining equation (3) & (5) gives:

$$U_T = \frac{J_g}{\varepsilon_g(1-\varepsilon_g)^{m-1}} + \frac{J_{sl}}{(1-\varepsilon_g)^m} \qquad (9)$$

Eq. (9) is derived assuming a uniform flow profile and uniform bubb1e concentration across the co1umn cross-section, meaning:

a) Small superficial gas velocities (1-3 cm/s)

b) Normal distribution of bubble sizes, variance (± 20%)

c) Small average bubble size (0.5-2.0 mm)

d) No liquid circulation (this is reasonable for column diameters less than 0.1 m)

For large columns, this is a reasonable assumption. For small columns, correction factors are required and given by Bhaga [22].

Jameson [23] derived that the first order flotation rate constant (k) is given by;

$$K = 1{,}5 * E_c \frac{J_g}{d_b} \qquad (10)$$

Where:

E_c ..... Collection efficiency, which is inversely proportional to the square of the bubble size.

In addition, it has been found that the rate constant was not related to the bubble size, gas hold up or superficial gas rate individually, but it was related to bubble surface area flux. For instance, for shallow froth the relationship was linear as;

$$K = P * S_b \qquad (11)$$

Where:

P..... Summarized the operational and chemical factors

Jameson showed that [23];

$$P = \frac{E_c}{4} \qquad (12)$$

2-1-11- Carrying Capacity

The rate of concentrate removal in terms of mass of solids overflowing per unit time per unit column cross sectional area is generally referred to as the carrying capacity of the column. This is related to the maximum

achievable coverage of air bubbles by particles and gives an upper limit to the capacity of flotation columns. Moreover, the capacity of a flotation column is limited by the amount of bubble surface available to carry the particles into the froth launder [24]. The concentrate solid flux Ca (tph/m²), in industrial columns, reches a value between 1-3 (tph/m²). This range depends on the level of wash water and the concentrate particle size [3].

2-1-12- Estimation of Carrying Capacity

At a given superficial gas rate and bubble loading there is a certain mass rate of solids that can be carried. A convenient unit is the mass of solid carried per unit time per unit column cross-sectional area, or carrying rate C_r, given by [16];

$$C_r = \frac{\pi K_1 d_p \rho_p J_g}{d_b} \qquad (13)$$

and,

$$C_{r,max} = \lim_{\substack{d_b \to 0 \\ J_g \to \infty}} \frac{\pi K_1 d_p \rho_p J_g}{d_b} \qquad (14)$$

In general, the loaded bubbles will exhibit a larger $d_{p,min}$ compared to the unloaded bubbles. The increase is usually small and the effect will not be pursued here [20].

Under normal column operating conditions, the quantity of solids carried over into the froth through entrainment is low due to the effect of wash water and can be neglected [24 & 25]. Furthermore, the size of particles is also small compared to the size of the bubbles, except in cases such as coal flotation. Under these conditions it can be shown that [26 & 27]

$$C = K.D_p \rho S_b \qquad (15)$$

Where C is the carrying capacity (tph/m²),

K is an empirical factor which accounts for the particle packing on the bubble surface

d_p..... is a characteristic diameter of the particle in the froth (mm),

S_b ..... is the superficial bubble surface area rate (surface area of bubbles passing through the column per unit time per unit cross sectional area)

ρ..... is the density of the particles in the froth (gr/cm³).

According to the equation (15), the carrying capacity for a given product can be increased by increasing the superficial bubble surface area rate, which in turn can be increased by increasing aeration rate or by reducing the bubble size.

It was also concluded, that in the normal range of operation, air rate and column diameter have only a marginal effect on carrying capacity [16, 28 & 29]

The maximum carrying capacity was related to the particle size and density of solids in the froth according to the equation [30];

$$C_m = 0.068\ d_p\ \rho \qquad (16)$$

Where:

C_m ..... is the maximum carrying capacity (gr/min/cm)

d_p ..... is the 80% passing size of solids in froth products (μm)

ρ ..... is the density of the particles in the froth (gr/cm³)

2-1-13- Column Height

The height of a column cell is determined by the required retention time, accounting for both short circuiting and a significant degree of froth dropback. In some cases, tall columns are undesirable. This arises when the feed grade is high and the floatable minerals have high flotation kinetics. This situation will cause the froth to become fully loaded and the retention time is decreses [30].

Rubinstein [8] has shown in fig. 2-10, that when the solids content of the feeds is relatively high (30%), the typical height of the collection zone adversely affects the processing capacity of the column. The literature suggests [31] that the phenomenon is due to the formation of aggregates with

high density, which may be entrained by the tailings discharge. According to this, it is recommended to use high columns to float fine particles (10 µm), and short columns for coarse particles (100 µm) [31]. Furthermore, Fig. 12 presents the results obtained by Maksimov et al., where is observed the existence of an optimal h_c/d_c ratio that maximizes recovery [32]. Maksimov et al. explains that when $h_c/d_c > 5$, the recovery may decrease as a consequence of the loss of overloaded bubbles to the tailings [32].

An explanation similar to that is given by Kawatra et al [31]. In spite of the apparent importance of these observations in column flotation, there are few studies oriented to characterize this phenomenon and to identify the experimental conditions that generate it.

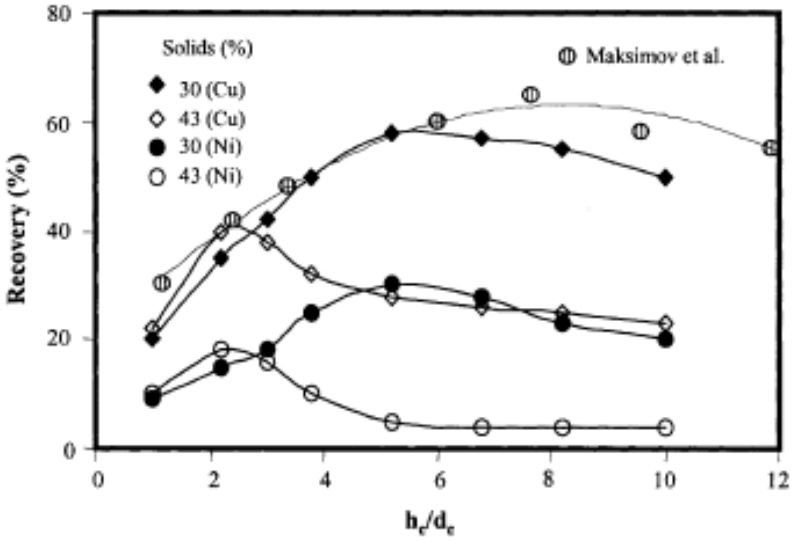

Fig. 2-10: Effect of the $\frac{h_c}{d_c}$ ratio upon recovery [31]

2-1-14- Hydrodynamics of Flotation Machines

There are two main factors influencing the flotation process is depends on; surface chemistry control and hydrodynamic conditions inside the reactor cell.

The surface chemistry control leads to attachment of the bubbles to the particle according to the potential conditions. Moreover, the hydrodynamic conditions provide the attachment development and the movement of particle- bubble to the froth [33].

2-1-15- Mixing Models

The particle collection process in a column is considered to follow first-order kinetics relative to solid concentration with a rate constant. The recovery of a first-order component process is dependent to rate constant, mean residence time and mixing parameters [16].

a) Plug Flow:

One of the mixing models is plug flow transport. As it is illustrated in fig 2-11, in this model, the residence time of all elements including fluid and minerals is the same. Moreover, in the plug flow transport, the concentration gradient of floatable mineral is along the axis of the column [16] and no mixing occurred in the flow direction. This type of flow is mostly equivalent to a batch processing system [34].

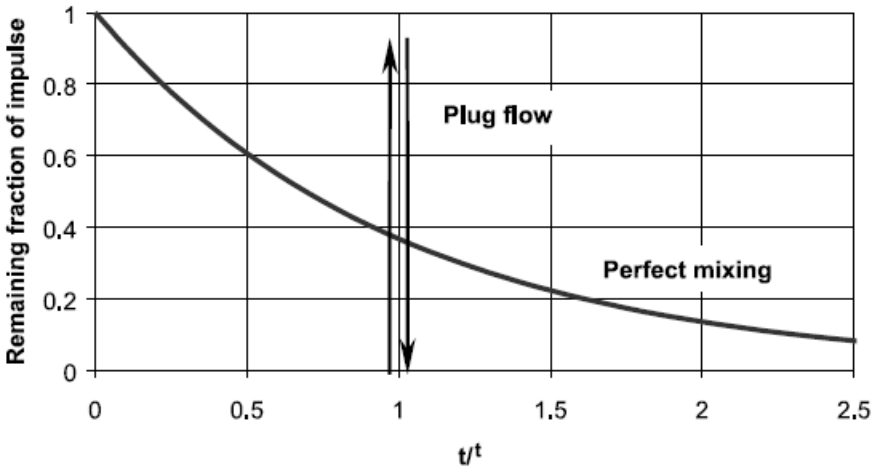

Fig. 2-11: Residence time distribution for plug flow and perfect mixing [34]

$$R = 1 - e^{-kt} \qquad (17)$$

Where;

k..... Constant rate

t..... Retention time (min)

R ..... Recovery (%)

b) Perfect Mixing:

Another extreme mode is a perfectly mixed reactor, where a retention time distribution exists and the concentration is the same throughout the reactor.

In this flow model, the tracer is dispersed in the whole volume of the device using a perfect mixing model and some of the tracer leaves the cell, while some would never leave. Therefore, there is a distribution of residence time from zero to infinity [34].

$$R = 1 - \frac{1}{1+k\tau} \qquad (18)$$

Where;

τ ..... Mean residence time (min)

In laboratory scale, using a typical laboratory flotation column (diameter by 5 cm and 5 to 10 m high), the approaches show a plug flow transport model, while in plant column is between plug flow and perfect mixing flow.

Transport conditions that do not approach either of the two extremes are usually described by one of two mixing models: tanks-in-series and plug flow dispersion. A row of mechanical flotation machines is well suited to tanks-in-series model and the flotation column. The plug flow dispersion model provides a good description of an axial mixing process in the collection zone.

Column dimensions can also be related directly to the plug flow dispersion model parameters, but not to the tanks-in-series parameters. Thus, a suitable model for the collection zone of a column, assuming a perfect radial dispersion, is an axial plug flow dispersion model [16].

By impulse injection of a tracer at the top of the recovery zone and measuring the concentrate of the tracer at a given distance below the

injection point, a function of turbulent mixing is obtained. The degree of mixing is quantified by the axial dispersion coefficient (E). Furthermore, by plotting the measured tracer concentration in the tailing stream against time (starting from the injection time) a residence time distribution (RTD) is achieved. The RTD can be modelled mathematically by using two parameters to describe the mixing conditions; the mean residence time and the vessel dispersion number [16].

$$N_d = E/(u * H_c) \qquad (19)$$

Where;

u..... Interstitial velocity (cm/s)

H_c..... Height of collection zone (cm)

E ..... A direct function of cell diameter [(unit of length)²/time]

N_d..... Vessel dispersion number (dimensionless)

$$E = 0{,}063 d_c \left(\frac{J_g}{1{,}6}\right)^{0,3}$$

2-1-16- Residence Time Distribution (RTD)

The efficiency is completely dependent on the time the material spends in the machine of a flotation as a dynamic process. The residence time distribution is the best indication of the flow pattern in the vessel.

The common way of RTD measurement is the injection of a tracer and thus the detection of the concentration of this tracer in the outlet(s) against time. The result of the distribution pattern is presented the ideal plug flow or the ideal perfect mixing types which are shown in fig. 2-12 [34].

From the experimental data, mean residence time τ and variance Ϭ² of the RTD are given by;

$$\tau = \frac{\sum t_j c_j \Delta t_j}{\sum c_j \Delta t_j} \qquad (20)$$

$$6^2 = \frac{\sum(t_j-\tau)^2 c_j \Delta t_j}{\sum c_j \Delta t_j} \quad (21)$$

$$\Delta t_j = {}^{(t_{j+1} - t_{j-1})}/_{2} \quad (22)$$

Where;

c_j ..... Tracer concentration

t_j ..... time (min)

$$6_r{}^2 = \frac{6^2}{\tau^2} \quad (23)$$

$6_r{}^2$ ..... Relative variance

An example of RTD diagram which is developed for WEMCO, Dorr-Oliver and Outokumpu industrial flotation cell is shown in fig. 2-12. In this investigation, a nuclear radiation material is used as tracer.

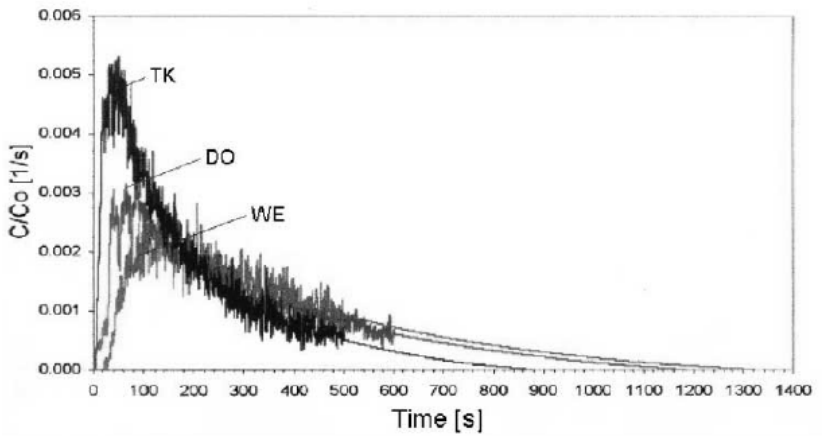

Fig. 2-12: Residence time distribution for liquid (Dorr-Oliver, WEMCO, Outokumpu Cells) [34]

When using the dispersion model, the feed and the discharge boundary conditions should be known. Sampling from the tailing stream outside the column satisfies the boundary conditions [16].

$$6_r{}^2 = 2N_d - 2N_d^2\left[1 - e^{\frac{-1}{N_d}}\right] \qquad (24)$$

and

$$u = \frac{H_c}{\tau} \qquad (25)$$

Bubble- particle collision probability models have been used to analyse the height issues [35 & 36]. Defining the minimum height in order to achieve at least one collision, the model shows that height is a strong function of particle size. Heights can increase from less than 1m for > 50 (µm) particles to more than 10 m for <10 (µm) particles. An engineering solution to the required height for a given process may develop from the work of Ityokumbul [37]. He proposed to replace the common kinetic approach with a mass transfer approach. This technique includes interaction between the collection and froth zones as froth dropback can dominate column design in some situations. To illustrate the need to consider these interactions, one possible argument against tall columns is that the bubbles become too loaded and this may reduce the solid carrying rate by overloading the froth in a manner similar to that when a column is overfed [16]. The decrease in recovery above a certain height observed by MAKSIMOV [32] may have its origin in this effect. However, the overfeeding phenomenon has never been explained. The capacity limitations, apparently imposed by the froth, have led to testing "Zero Froth Column Flotation".

2-2- Previous Case Studies

a) Generally, flotation in column cells has been simulated with models based on the mixing characteristics prevailing in the cell [30]. For example, Finch and Dobby [16] have proposed the axial dispersion model to describe the mixing conditions of laboratory columns (2.5–10 cm of diameter) and industrial columns (up to 2.5 m diameter). According to this model, the

knowledge of the mixing conditions helps to identify the relationship between both grade and recovery and operational parameters such as nominal residence time and relative flow rates of column streams. In this theoretical approach, the height of the column, directly related to the residence time, improves the mineral collection up to a point, where the collection is limited by the carrying capacity (surface bubble saturation) instead of being dictated by the flotation kinetics. The effect of the column height on the flotation performance has been studied from an experimental approach [36]. According to the authors, for a given capacity of the column and constant feed flow rate, the recovery decreases and the grade increases when the hc/dc ratio increases. Moreover, the authors suggest that it is necessary to have a separation between the sparger and the tailing discharge, to prevent the loss of the mineralized bubbles to the tailings stream.

b) In the investigation of a flotation column of an inside diameter of 15 cm and a total height of 8 m, all streams handling is achieved using Masterflex peristaltic pumps. The pulp is prepared in a 250 lit capacity conditioning tank, and is then transferred to another 250 lit tank, for continues operation. The column feed port is located about 180 cm from the column overflow lip. The concentrate overflows into a concentric launder measuring 25 cm in diameter by 34 cm in tallest side height. The overflow is also drained by gravity continuously [39].

Air is injected at the bottom of the column through a stainless steel sparger, whereas wash water is sprayed over the overflowing froth via a copper tube. Air and wash water flow rates are measured by an MKS mass flow meter and a turbine flow meter. Feed, tailing and concentrate flow rates are measured using magnetic flow meters.

Pulp- froth interface and bias rate are estimated from a conductivity profile measured using eleven ring type stainless- steel electrodes mounted flush against the inner wall of the column upper section. The various pairs of electrode are sequentially excited to avoid current propagation between the pairs [39].

c) The experimental program was conducted in a laboratory column (0,057 m dia. & 4,5 m height), made of transparent acrylic tube. Actually,

the total column height was constant but the modification of the height of the collection zone was easily accomplished, using a movable sparger (stainless steel, 2 μm pore size). This sparger was suspended in the centre of the column by a 3 mm OD vinyl air supply tube. The slurry is feed to the column at 1.04 m from the overflow lip [30].

Others accessories of the column rig are a froth depth controller, a pH meter (Omega 5T96), a conductivity meter (Orion model 162), a pulp temperature controller and a photographic camera. This camera was installed in front of the screen column section.

The mineral used to prepare the flotation pulp was silica sand with a size distribution between 50 and 300 μm (d_{80} = 190 μm).

The experiments were performed in a closed circuit, with the aim to keep the tailings flow rate (J_t) constant, wash water flow rate (J_{ww}), gas flow rate (J_g) and froth depth (h_f) at 1- 0,16- 1.46 cm/s and 0.3 m, respectively [30].

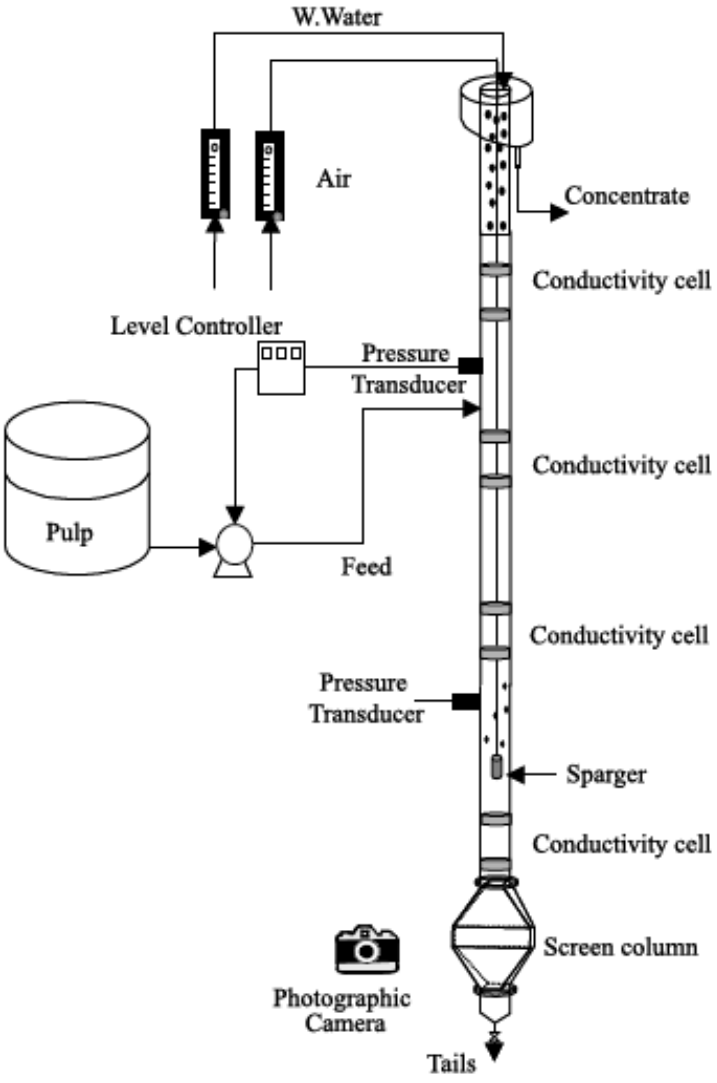

Fig. 2-13: The laboratory column flotation [30]

d) The design of the semi-batch column is based on column flotation practices and the concept of air lifting to keep solid particles suspended as in Pachuca tanks [40]. The device, shown in Fig. 2-14, consists of an outer column (measuring 75 cm tall * 7 cm dia.) and an inner column (measuring 15 cm tall * 3.8 cm dia.), both made of transparent plexiglass. Pulp continuously flows up the inner column and down the annual space between the two columns, thus providing the necessary retention time in a relatively short column [40]. This manner of pulp circulation is achieved by injecting compressed air into the inner column through a sparger which at the same time provides the gas bubbles required for flotation.

A hemispherical baffle is installed at a distance of 2 cm above the inner column for the purpose of preventing the slurry stream from directly shooting up into the froth phase above. The baffle has 2.5 mm holes punched onto its surface. Located at the top, typically 5 cm above the froth surface a wash water sprayer in the form of a hollow ball is located. The semi-batch column may be equipped with various auxiliary devices such as peristaltic pumps, air flowmeter, solenoid valves, and pH meters [40].

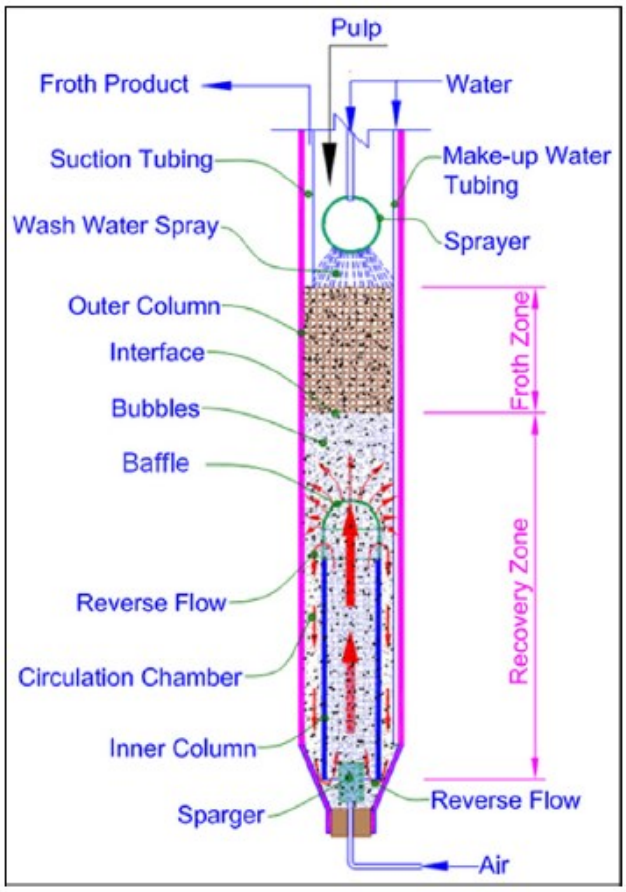

Fig. 2-14: Schematic of the Semi-Batch Column [40]

The main operating variables of the semi-batch column include froth thickness, pulp density, air flowrate and the amount of wash water. The froth thickness was studied in the range of 5 cm to 30 cm, the pulp density in the range of 10–35%, and the air flowrate in the range of 0.94–3.78 lit/min. The column was operated with a pulp volume of 750 ml, and a flotation time of 3 min was applied in all tests. All three parameters were found to

significantly influence the flotation results, with the air flowrate having the most impact. The froth wash water, which was applied at a rate of 440 ml/min in continuous mode and 1900 ml/min in intermittent mode, was instrumental in obtaining cleaner froth products, as well as improving the selectivity. It is recommended that for any given application, these variables be carefully investigated and optimized [40].

e) The laboratory column cell was used for de-inking of waste paper with 10 cm diameter and 470 cm length. The column was operated with different sparger systems as porous stainless steel, filter cloth and jetting spargers. The changed variables in the experiment were, the range of gas rate, the retention time, froth depth and column height [41]. The gas rate was accurately measured and controlled with a mass flow meter. Gas hold up was measured by both pressure and conductivity method and the permitted bubble size was estimated by drift flux analysis [42]. Data from the three different sources are plotted together in Fig. 2-15. A linear relationship is observed with a 95% relative confidence interval on the slope of ±3%.

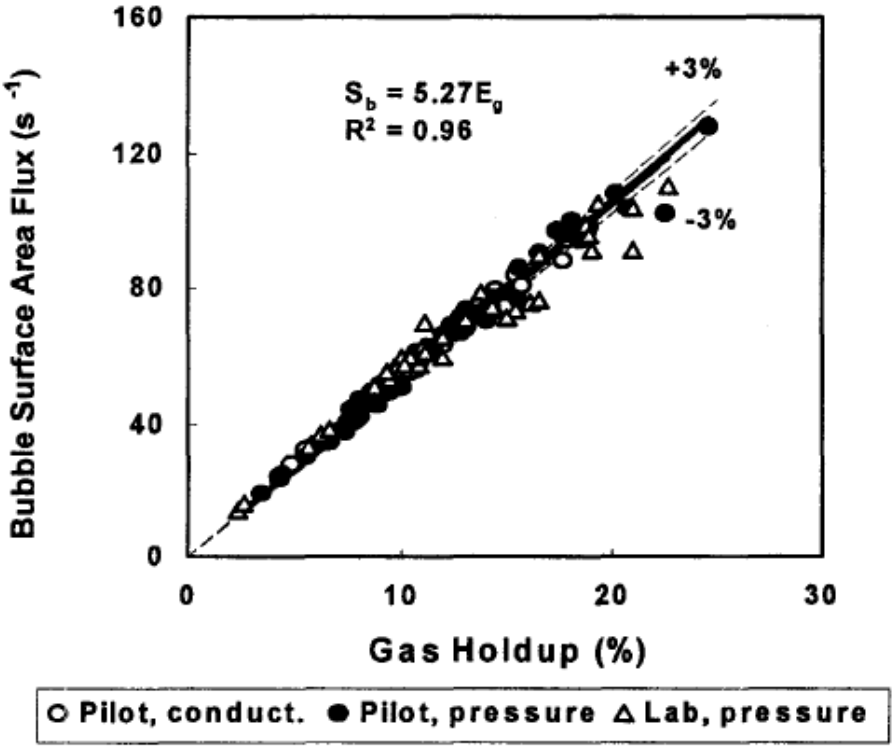

Fig. 2-15: Bubble surface area flux and gas holdup in pilot and lab flotation columns used for de-inking [42].

Chapter Three:

Montan Column Flotation Cell

3- Montan Column Flotation Cell

The cell has been designed and constructed according to several desire demands and limitations of equipment.

A Free student version of AutoCad Inventor software is used to draw a primary model of the cell with all details and dimensions. The cell is including several parts to be accessible and easy to assemble and disassemble such as; foam launder, the "Main Upper" part, middle main part, feed inlet, conical bottom part, bubble generator, bubble generator holder and outlet pipes for pressure measurement.

3-1- Foam launder

The foam launder, which has an inner diameter of 153,6 mm, is constructed to collect the overflow foam at the top of the cell and is shown in fig 3-1. The height of the launder is between 73,81 mm and 166,19 mm. The bottom of the launder has a 30° incline. The details are referred in appendix 1.

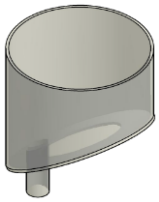

Fig. 3-1: Foam Launder

3-2- Main upper and middle parts

The main flotation chamber has an 81,4 mm inner diameter, of a 4,3 mm thickness, 300 mm height of the upper part and 1160 mm height of the middle parts. The details are illustrated in appendix 2.

Fig. 3-2: Main upper and middle part

3-3- Feed port

The feed port pipe is placed in the main body of the flotation chamber for a better distribution of the feed suspension through the cell. The feed pipe which has an inner diameter of 32 mm, is prepared with a cut at the top that gives two purposes; having laminar flow of fresh feed suspension in the flotation chamber and to distribute the suspension around the main vertical axis of the cell. The dimension are given in appendix 3.

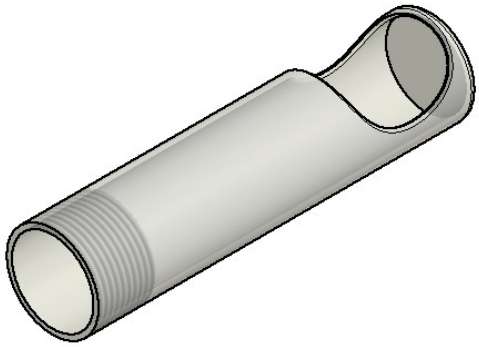

Fig. 3-3: Feed port

A schematic view of the assembled feed port is shown in fig 3-4. A complete view with details is given in appendix 4.

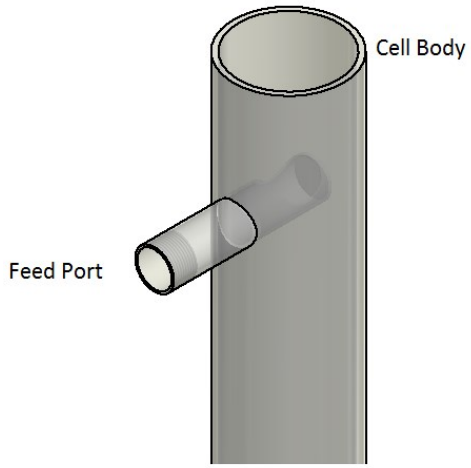

Fig. 3-4: A view of the assembled feed port on the main cell body

3-4- Conical bottom part

The designed conical shape part which is shown in fig 3-5 and appendix 6, is placed at the bottom of the cell.

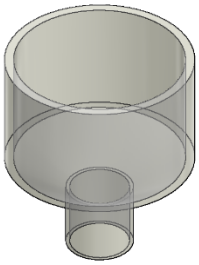

Fig. 3-5: Bottom conical part

3-5- Bubble generator

In order to disperse the bubbles through the cell, a porous tube bubble generator is located in the cell near to the bottom. In principle, with injection of compressed air through the bubble generator, the tube is expanded. Therefore, the small holes are expanded in the texture of the tube and bubble are released into the cell. The bubble generator, which produced by Eriez company, is shown in fig. 3-6.

Fig. 3-6: Bubble generator

3-6- Bubble generator holder

One of the challenges during the design of the column was the structure of the connections between the bubble generator, the cell body and the compressed air pipe inside the cell. As bubble generator holder, a triple pipe is used to keep the bubble generator synchronize with the main vertical axis of the cell. The triple pipe, which is made of PVC-U polymer, is connecting compressed air supply to the bubble generator. The holder is shown in fig 3-7. This part is assembled near to the bottom of the cell. The details are given in appendix 7.

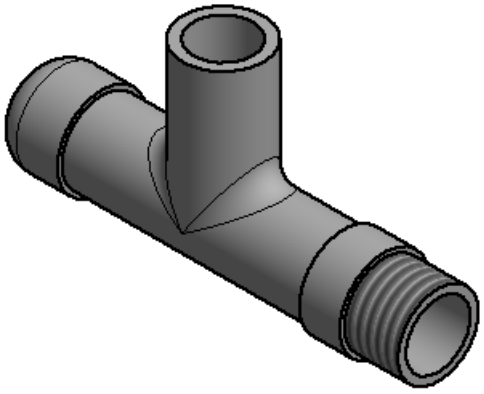

Fig. 3-7: Bubble generator holder

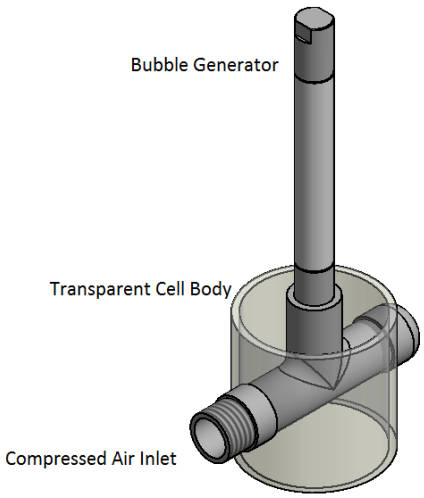

Fig. 3-8: A schematic view of the bubble generator assembly

3-7- Outlet pipes for pressure measurement

There are two outlet pipes situated on the main cell body between the feed port and the bubble generator holder to measure pressure difference. This measurement is used for the gas holdup calculation. The outlet points are shown in fig 3-9 and appendix 4.

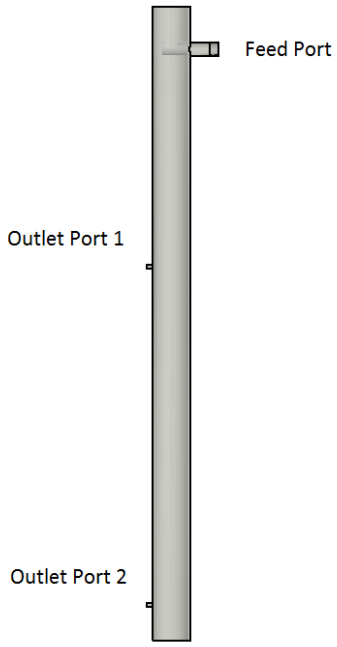

Fig. 3-9: Outlet pipes for gas holdup measurement

3-8- Connections

Regarding to connect the mentioned parts of the cell, a screw connector type is used. This type of connector is chosen, because it is easy to assemble and disassemble. The details of the connector and dimensions are given in appendix 9.

3-9- Cell assembly

In conclusion, the constructed column cell (fig. 3-10) has following characteristics as shown in table 3-1:

Table 3-1: Montan column cell characteristics

Charactristic	Value
Cell height	182 cm
Cell diameter	81,4 mm
Cell volume	9,5 lit
Distance between gas holdup measurment outlets	80 cm
Maximum air pressure for bubble generator	1 bar
Minimum air pressure for bubble generator	0,25 bar

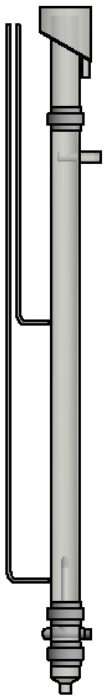

Fig 3-10: schematic view of final column designed

3-10- Conditioning tank

In order to prepare the feed slurry of the column, a barrel with 50 litre capacity is used. Dry solid material, water and reagents are mixing in the conditioning tank at desired solid content and a sequence of additives and pH adjustment. Furthermore, a variable speed impeller is used to prepare the pulp.

The amount of added water into the barrel is controlled by a water flowmeter.

Fig. 3-11: Conditioning tank

3-11- Cell Control Procedure

To mix and prepare the feed suspension, a barrel with 50 lit capacity and an electrical mixer are used as conditioning facilities. After mixing and preparation of the feed pulp with desired reagents, the suspension is fed into the cell to the desired level. At this time the discharge and air valves are close. The desired level of suspension is adjusted until it reaches a level some centimetres above the feed port to have enough depth of foam at the top of the cell. Then, the discharge valve is opened to have a constant suspension level in the cell. On the other hand, the income and outcome flowrates must be equal. At this time, the air valve is opened to penetrate bubbles through the column cell. As all used valves are controlled manually, the adjustment of the operating condition such as input and output flowrates are difficult and time consuming. To control the flotation column system, accurate alterations of different parameters are important and have a large impact on the cell´s performance.

A digital flowmeter is applied for feed flowrate determination. Based on the digital flowmeter manual, the pipe at the location of flowmeter installation must be full of suspension for a correct flowrate measurement. For investigation reasons, it was necessary to run some experiments at lower flowrates. In these cases, the digital flowmeter does not work properly. Thus, the feed flowrate was adjusted at the desired flowrate by measurement of suspension volume against time.

After each test, all containers and pipes must be cleaned to avoid chocking.

As a summary, the instructions for the column cell are shown in fig 3-12 and the test implementation procedure is described step wise as following:

1- The conditioning tank is filling with water for the feed flowrate adjustment. At this time, all valves are closed except valves 1 and 2. As a next step, valve number 2 is opened fully and the feed flowrate is set to the desired flowrate by adjusting of valve 1. From now on, valve 1 will not manipulated any more.

2- All valves, except valve 1, are closed to prepare the feed suspension with a desired solid content in the conditioning tank.

3- Valve 3 is opened full to charge the column cell to the desired level (usually some centimetres above the feed port). At this time, valve 5 is regulated as well to the desired wash water flowrate.

4- After achieving to the desired pulp level in the column cell, valve 7 is opened carefully to reach a constant level of suspension in the cell.

5- The air valve (valve 4) is opened to introduce air bubbles into the flotation cell.

6- the system is cleaned after experiment with water.

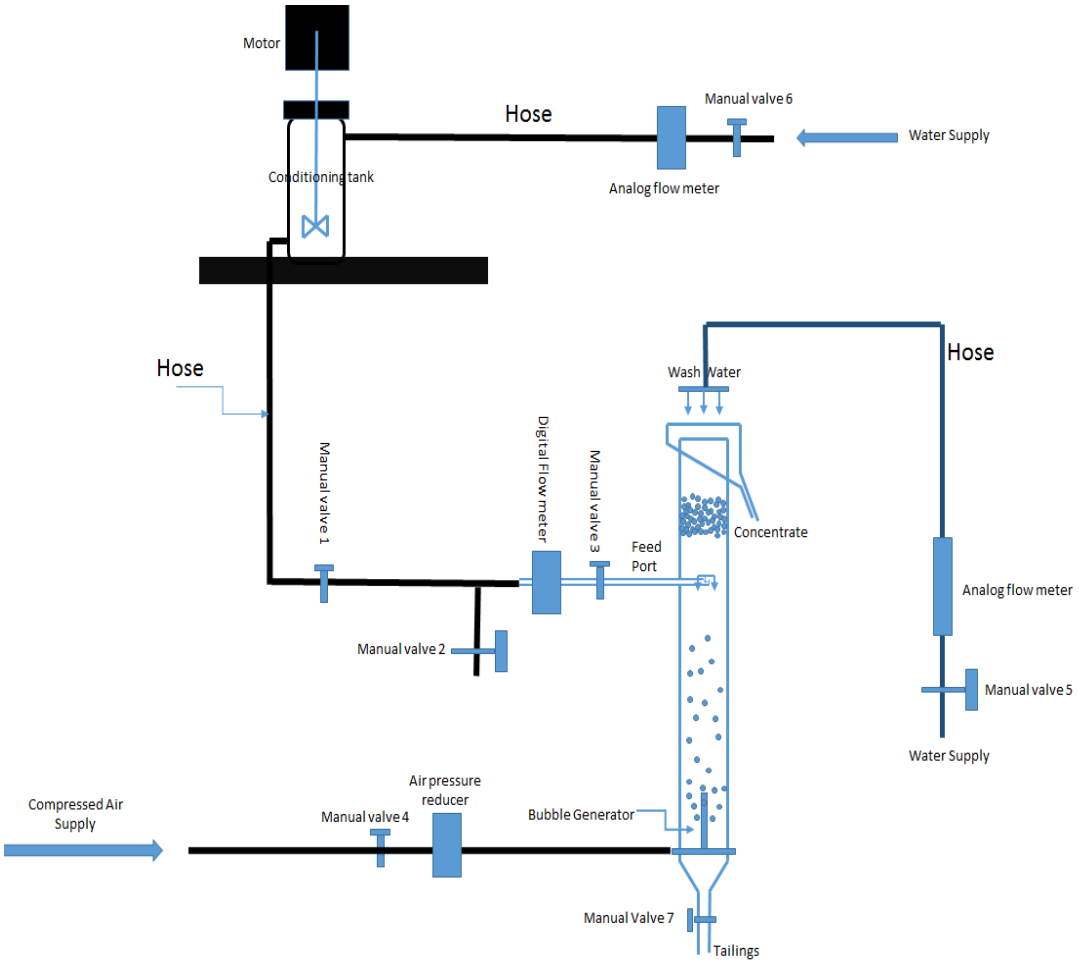

Fig. 3-12: Schematic view of the column flotation cell and related facilities

Chapter Four:

Experimented Material

Graphite and talcum ore have been chosen as testing material for the constructed cell. The reason for selecting these types of material are summarized below:

1- Having natural hydrophobicity property (easy to float)
2- Previous knowledge about the characteristic and mineralogy of material
3- Enough amount of sample validity in the sample storage
4- Being easy to evaluate the products content via LOI and density measurement.
5- Ban of chemical reagents usage

4-1- Graphite

4-1-1- A summary to graphite formation and structure

Graphite is a natural formation of crystalline carbon. As a mineral, graphite forms when carbon is buried in the earth crust and in the upper mantle under defined pressure and temperature. Graphite, which was anciently referred to as Plumbago, is one of the allotropes of carbon, semimetal and known as highest grade of coal. The phase diagram in fig. 4-1 indicates the temperature and pressure condition of graphite formation.

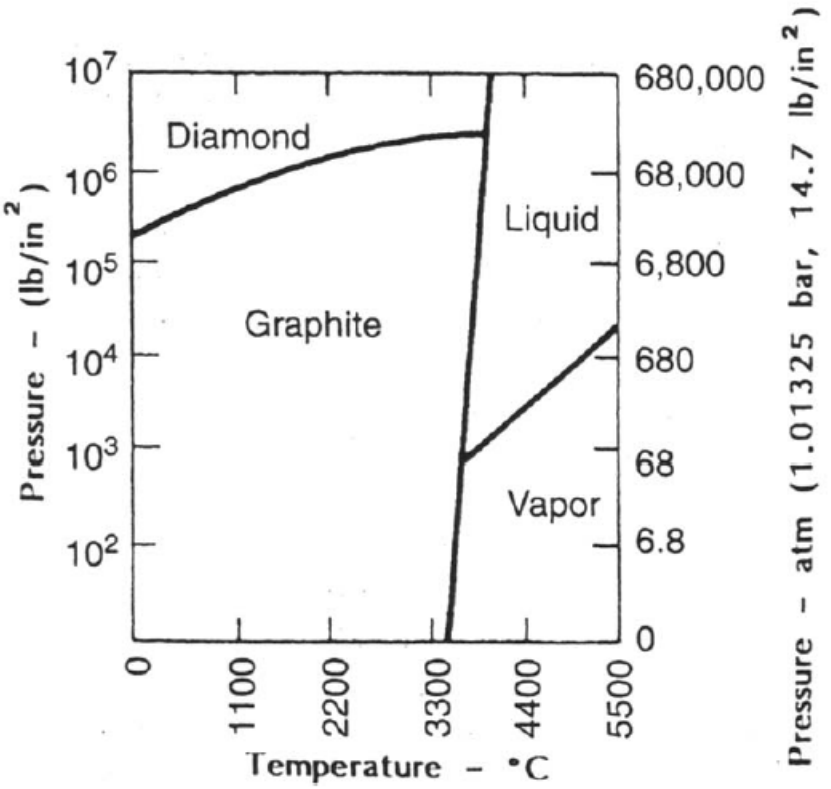

Fig. 4-1: Graphite phase diagram [43]

Carbon forms a complex compound with hydrogen and other minerals which are the basic of organic chemistry.

The structure of graphite consists of stacks of six-membered rings in a sheet-like structure. Three neighbouring atoms are arranged at the apices of equilateral triangles. In each carbon atom, three of four valance electrons must be locked in tight covalent bonds with the three close neighbours. The remaining electron is free to migrate across the surface of the sheet. This structure provides the ability of graphite to be highly electrical conductive. The graphite acts rather as a metal [43].

The distance between the sheets is slightly bigger than an atom diameter and is calculated at 0,34 nm. The Van der Waals bonding between the stacks is very weak and perpendicular to them. Having such an open structure implies that the occupied space of the total available space is only 20 %, thus accounting for the relatively low density of graphite.

Physical features of graphite [43]:

- Apart from the perfect diagnostic basal cleavage, other cleavage planes have been identified.
- The hardness property of graphite lies between 1 and 2 according to Mohs´ scale
- Graphite has mark paper and soil fingers properties
- The density is between 2,09 gr/cm³ and 2,23 gr/cm³ (lighter than its paramorphism diamond at 3,52 gr/cm³.
- The color is varying from shining black to dull.
- Graphite has high electrical conductivity property parallel to the sheets and semi-conductivity property perpendicular to the atomic carbon sheets
- Graphite is transparent to X-rays.

The main difference between graphite and diamond is that the carbon bonding involves sp^3 hybridization in diamond and sp^2 hybridization in graphite. As a result, diamond has three-dimensional crystal structure, whereas graphite consists of carbon layers with covalent and metallic bonding within layers. The electrical conductivity property of graphite leads to use as electro-chemical electrodes. As a result of this anisotropy, the carbon layers can slide with respect to one another quite easily, thus making graphite a good lubricant and pencil material.

Graphite generally occurs as a result of metamorphism of organic matter in sediments. As metamorphic grade increases, carbonaceous material converts to amorphous graphite [44]. Vein graphite is assumed to form by partial volatilization of graphite and subsequent recrystallization during regional granulite and / or charnockite faces metamorphism. Amorphous graphite is generally considered to have originated by thermal or regional metamorphism of coal or carbonaceous sediments [43].

Impurities include minerals as for instance, quartz, mica, calcite, feldspar, amphibole, garnet, with occasional amphiboles, pyrrhotite, magnetite and magnetite.

Graphite is used mainly for lubricants, pencils, batteries, brake lining, conductive coatings, bearing, refractories and crucibles.

4-1-2- Processing of Graphite

According to the mentioned graphite structure, gangue minerals and property descriptions, density separation, electrostatic separation and flotation can be variable options of beneficiation wit regard to mineral processing. Other conditions such as intergrowth and particle size distribution must be considered for processing method selection as well.

Graphite can easily be enriched by flotation because of its high natural hydrophobicity properties, especially in the small particle size range. As collector, kerosene, paraffin, diesel oil, fuel oil or ionic collectors like potassium amyl xanthate, dithiophosphate are commonly used. As frother, pine oil or MIBC (Methyl isobutyl carbinol are used. Sodium silicate, quebracho and starch are used to depress gangue minerals [43].

4-2- Talc

Talc is a widely used industrial mineral, which is composed of hydrated magnesium sheet-silicates with a theoretical formula of $Mg_3Si_4O_{10}(OH)_2$ that belongs to the phyllosilicate family [45]. Talc applications including ceramics, cosmetics, pharmaceuticals, paints, plastic, paper, roofing felt, insecticides, rubber and others. For each case of talc application, various degrees of purity are required. For instance, low grade talc is used as a filler in drywall sealing compounds, medium grade finds its application in paper industry and high grade is mainly required in cosmetic and pharmaceuticals. Most applications need fine grained talc and a minimum of asbestiform particles [46].

Talc consists of a two dimensional sheet structure forming two layers of silica tetrahedral held together with octahedral brucite [47]. Talc surface is comprised of two types of surface area, the basal cleavage faces and the edges. It is believed that the talc faces are non-polar and hydrophobic because, the faces surface has no charged group, whereas the edges are hydrophilic due to the presence of charged ions (Mg^{2+} and OH^-). The major gangue minerals of talc are carbonates, magnesite, dolomite, serpentine, chlorite and calcite, which contribute to undesirable characteristics. The trace minerals include magnetite, pyrite, quartz and tremolite. The

percentage of some constituents in talc such as calcium oxide, iron oxide and aluminium oxide determine the quality of talc samples for market demands [48].

Chapter Five:

Column Cell Flotation Experiments & Results

The performance of the constructed cell was evaluated by flotation experiments with the talc and graphite ore. Moreover, some of the operation parameters were measured during these experiments such as the bias rate and the gas holdup. The procedure of the tests and the evaluation methods are described as following.

5-1- Material evaluation

To characterize the flotation products competitively, simple and quick, the density and LOI measurements were used.

5-1-1- Density measurement

During all the experiments, the solid density has been measured by helium pycnometer which is provided by micromeritics company model AccuPyc 1330. The helium pycnometer measures the volume of sample in the sample cup. The measurement principle is based on the ideal gas equation (equation 26) using the measurement of pressure to determine the volume of a sample.

$$PV = nRT \qquad (26)$$

Where;

n..... number of mole of gas (mole)

R ..... universal gas constant (R= 8,314 $\frac{J}{K.mol}$)

V ..... volume (cubic metres)

P..... gas pressure (pascal)

T ..... temperature (Kelvin)

5-1-2- Loss of ignition (LOI)

The LOI test was used for both the graphite and talc ore samples for products evaluation, but under different conditions. In both cases, the usual and standard procedures were used for each type of sample.

a) LOI test of graphite ore

Has been carried out with around one gram of dry sample in the ceramic sample cup. The experiment was performed on the graphite ore material as received. The particle size of sample was determined at 100% -100 µm. At first, the sample was heated up to 425 degree Celsius in the furnace for two hours. At this temperature, the sample release the moisture. Preheating of the sample leads to measurement of the carbon content more accurate. The stepwise procedure of the LOI test for graphite ore is explained as follow:

- Measurement of sample mass in the cup.
- Preheating to 425 degree Celsius for two hours.
- Sample mass measurement
- Heating at 1025 degree Celsius to oxidize carbon content for 8 hours
- Mass measurement of burnt sample.

b) LOI test for Talc

The used sample mass, as same as graphite, is around one gram in the ceramic sample cup. The sample was heated up at 1050 degree of Celsius for one hour.

5-1-3- Determination of carbon and sulphur content

LECO Company is the supplier of the apparatus for carbon and sulphur content measurement. Therefore, this method of carbon and sulphur analysing is known as “LECO” method. This experiment was carried out only on the products of the column flotation test with talc ore. In principle,

the sample is combusted at high temperature so that all the carbon and sulphur contained oxidized to CO_2 and SO_2 form, respectively. The device is equipped with an infrared detector to record the concentration of CO_2 and SO_2 [49].

5-2- Talc sample characteristics and preparation

The talc ore sample originates from Gemersha Polowa mine, which is located in Slowakia. In table 5-1, the particle size distribution, LOI and density values of each fraction, according to the described procedures in section 5-1-1 & 5-1-2, are illustrated. As sample preparation for LOI and density measurements on coarse fractions (+200 µm), the sample was ground by mortar and pistil to achieve a suitable particle size for measurements.

Table 5-1: Result of manual screen analysis as well as LOI and density measurements in size classes

Fraction (µm)	Mass (gr)	Mass (%)	Cum. Passing (%)	LOI (%)	Density (gr/cm³)
+8000	132,7	3,3	96,7	14,30	2,86
+6300-8000	356,2	8,9	87,7	15,12	2,83
+4000-6300	683,8	17,1	70,6	15,06	2,86
+3150-4000	276,0	6,9	63,7	14,91	2,85
+2000-3150	490,6	12,3	51,4	15,94	2,86
+1250-2000	414,4	10,4	41,0	16,21	2,89
+710-1250	417,4	10,5	30,5	15,41	2,88
+500-710	218,0	5,5	25,1	15,41	2,89
+315-500	245,0	6,1	18,9	15,40	2,88
+250-315	110,2	2,8	16,2	15,08	2,89
+125-250	248,4	6,2	9,9	14,34	2,89
-125	396,6	9,9	0,0	10,87	2,87
SUM	3989,33	100	Ave.	14,87	2,87

Based on the microscopic investigations on the talc ore in the particle size range of -63+40 μm, quartz and dolomite are encountered as the main gangue minerals apart from pyrite. For the nominal (modal) composition, all the carbonates are calculated as dolomite. From the known carbon and sulphur content of the dolomite [$(CaO)(MgO)(CO_2)_2$] and pyrite [FeS_2] and the measured carbon and sulphur content in the sample, the total content of dolomite and pyrite were estimated. The nominal loss of ignition of pure talc is given by 4,75% [48].

From the decomposition reaction of dolomite, which is;

$(CaO)(MgO)(CO_2)_2 \rightarrow (CaO)(MgO)+2CO_2\uparrow$

and pyrite oxidation reaction, which is

$FeS_2+11O_2 \rightarrow Fe_2O_3+4SO_2\uparrow$

The relative weight loss of dolomite related to carbon content (4,02 gr/gr of carbon) and the relative weight loss of pyrite related to the sulphur content (0,626 gr/ gr of sulphur) were calculated. Thus the nominal mineral system was resolved from LOI and density measurement as well as the carbon and sulphur contents in the following way. The mineralogical composition within the size classes was determined by a combination of physical and chemical analysis. The physical analysis included

- Manual sieve analysis of a sample
- Fraction +10 mm was subdivided into density classes by sink-float analysis.
- Particle density measurement
- LOI measurement

The density of pure minerals were determined by the helium pycnometer on manually collected samples of pure minerals (mineral standards). The results are given in table 5-2.

Table 5-2: Density of pure minerals [50]

Mineral	Density
Pyrite	5,20 gr/cm³
Dolomite	2,963 gr/cm³
Talc	2,792 gr/cm³

The LOI value of the minerals were determined on ground samples in the furnace by heating at 1050 degree of Celsius for one hour.

The analysis results of carbon and sulphur content, by combustion at high temperature followed by infrared detection of CO_2 and SO_2 on the dolomite and talc standard are given in table 5-3.

Table 5-3: Carbon and sulphur content analysis of dolomite and talc standard [50]

	Carbon content (%)	Sulphur Content (%)
Dolomite	12,7	0,05
Talc	0,29	0,01

The particle of fraction +10 mm were measured for particle density, subdivided into density classes and prepared for carbon and sulphur analysis by comminution.

The size classes +2-4 mm, +1-2 mm, +0,5-1 mm, +0,315-0,5 mm, +0,2-0,315 mm were analysed by sink-float analysis at 3,12 gr/cm³ liquid density [50].

The applied equations in table 5-4 are as follow:

Dolomite Content= Carbon Content/0,1302 (27)

Pyrite Content= Sulphur Content/0,5306 (28)

$LOI_{Calculated}$ = 4,02*(Carbon content)+ 0,626*(Sulphur content) (29)

$$LOI_{residue} = LOI_{measured} - LOI_{calculated} \quad (30)$$

$$\text{Talc content} = (LOI_{residue})/0{,}0475 \quad (31)$$

Residue Mineral Content= 100- Talc content- Dolomite content- Pyrite content

Table 5-4: Mineralogical investigation of talc sample [50]

Size Classes (mm)	Density Classes (gr/cm³)	Mass (%)	Density (gr/cm³)	LOI (%)	Carbon Content (%)	Sulphur Content (%)	Calculated LOI (%)	Meas. LOI - Cal. LOI (%)	Mineral Composition			
									Talc (%)	Dolomite (%)	Pyrit (%)	Rest Minerals (%)
+10	2,39-2,65	4,32	2,72	5,91	0,560	0,750	2,72	3,19	67	4	1	27
	2,65-2,70	4,94	2,66	1,11	0,160	0,060	0,68	0,43	9	1	0	90
	2,71-2,75	8,02	2,76	4,91	0,500	0,004	2,01	2,90	61	4	0	35
	2,76-2,80	30,25	2,76	7,9	1,240	0,080	5,03	2,87	60	10	0	30
	2,81-2,85	29,01	2,80	7,83	0,890	0,600	3,95	3,88	82	7	1	10
	2,86-3,25	23,46	2,85	12,68	2,580	2,460	11,90	0,78	16	20	5	59
+4-10		23,38	2,81	7,09	0,875	0,477	3,81	3,28	69	7	1	23
+2-4		12,05	2,79	8,87	1,170	0,098	4,76	4,11	87	9	0	4
+1-2		12,05	2,79	8,35	1,140	0,056	4,61	3,74	79	9	0	12
+0,5-1		4,22	2,81	8,46	1,180	0,049	4,77	3,69	78	9	0	13
+0,315-0,5		3,23	2,79	8,52	1,180	0,027	4,76	3,76	79	9	0	12
+0,2-0,315		3,33	2,79	8,26	1,070	0,016	4,31	3,95	83	8	0	9
-0,2		12,47		7,1	0,670	0,130	2,77	4,33	91	5	0	3

The results were checked by back calculating the density of the size classes and comparing them to the measured density. From those size classes, split into the density classes -3,126 gr/cm³ and +3,126 gr/cm³, also the liberated pyrite content could be estimated taking the mass of the heavier fraction as free pyrite. The results are given in table 5-5 [48].

Table 5-5: Mineral composition of talc sample and density back calculation [50]

Talk (%)	Dolomite (%)	Intergrowth Pyrite (%)	Free Pyrite (%)	Back calculation of density (gr/cm³)	Relative deviation (%)
85,22	8,85	0,18	1,52	2,82	1,01
76,95	8,57	0,10	2,18	2,81	1,29
76,11	8,88	0,09	2,04	2,81	1,22
78,24	8,95	0,05	1,27	2,80	0,87
82,35	8,13	0,03	1,05	2,80	0,78

Regarding to the talc ore sample preparation for flotation test, the sample was ground by the vertical roller mill (VRM 200 A&V) at the laboratory of mineral processing at defined settings. The mill was operated in open circuit with an air classifier to discharge the particle at the maximum particle size of about 200 µm. Settings were chosen in order to obtain a fine product of low LOI (< 8%). The coarse particle material containing liberated pyrite in a fraction of +200 µm was stored for further upgrading making use of differential breakage behaviour. The mass recovery of fine fraction, the recovery based on LOI and recovery based on density values were calculated as 23,85 %, 22,72 % and 25 %, respectively.

The general mill´s characteristics and settings are illustrated in tables 5-6 and 5-7.

Table 5-6: VRM 200 Characteristics

Mill type	Vertical roller mill
Maximum throughput	100 kg/hour
Diameter of plate	200 mm
Nominal power draw of motor to rotate the plate	5 KW
Number of rollers	2
Roller diameter	13 cm
Nominal ventilation power	18 KW
Classifier´s cage diameter	15 cm
Maximum rotational speed of cage	4000 rpm
Cut size with nominal air volume (1000 m^3/h)	50 µm

Table 5-7: Mill settings for talc sample grinding

Feed flowrate	20 kg/h
Plate rotational speed	65 rpm
Roller downward pressure	15 bar
Distance between rollers and plate	3 mm
Roller upward pressure	11 bar
Ventilator rotational speed	1500 rpm
Classifier´s cage speed	1500 rpm

Table 5-8 shows the data obtained from four series of sampling during comminution. The samples were taken from coarse and fine streams of the air classifier for a duration of 220 sec. The reason for selection of 220 sec as the sampling duration was the air classifier filter. The filter of the air classifier contains four filter batteries and every 55 seconds, the battery changes for discharge. To obtain a representative sample, the samples were taken from a complete filter cleaning circuit.

Table 5-8: Data of obtained samples from comminution operation

	Series 1	Series 2	Series 3	Series 4	Ave.
Fine Product Mass (kg)	0,851	1,0595	0,9875	1,0105	0,977
Coarse Product Mass (kg)	4,0025	4,101	4,1335	4,151	4,097
Yield (%)	21,26	25,84	23,89	24,34	23,85

A schematic view of the mill and streams is shown in fig. 5-1.

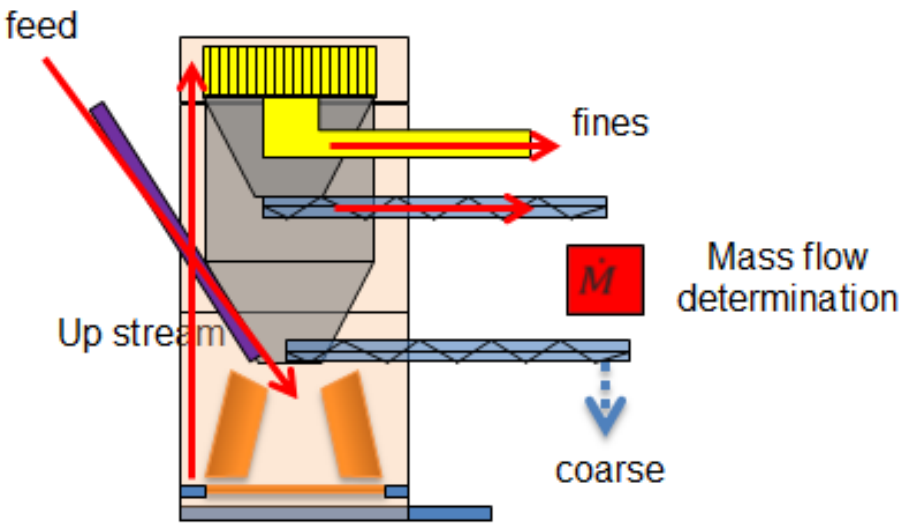

Fig. 5-1: Schematic view of vertical mill

The milling process comprises grinding and air classifying in two shapes. Fig. 5-2 is illustrating these processes schematically. The mill was operated in open circuit with the air classifier to make use of the differential breakage behaviour of the different minerals. In open circuit, the coarse material from the classifier was relived from the mill via a spiral conveyor (grid bypass system). Therefore, a pre-beneficiation is implemented during comminution and classification.

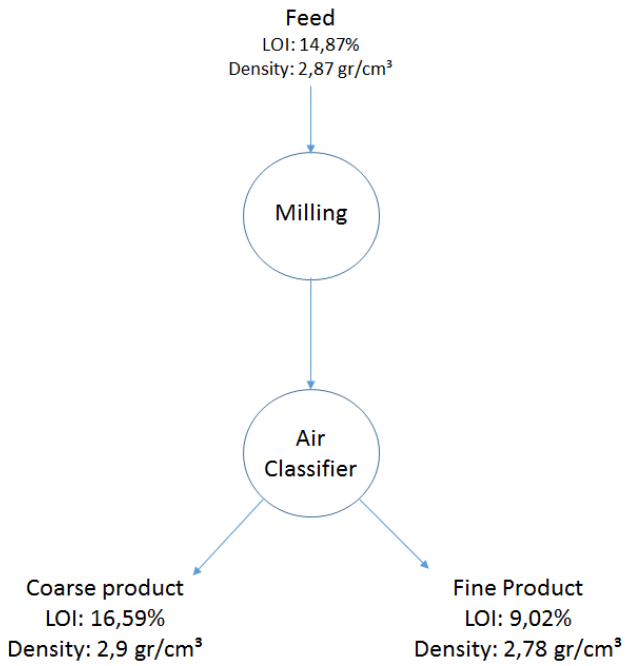

Fig. 5-2: Sequence of processes in the vertical roller mill

Tables 5-9 and 5-10 show the particle size distribution (PSD) of coarse and fine fractions of the mill, respectively. The size distribution diagram is also illustrated in fig. 5-3.

Table 5-9: VRM200. Result of screen analysis of the coarse fraction of the mill product

Size(µm)	Mass (gr)	Mass (%)	Cum. Passing (%)
+1000	2,96	1,29	98,71
+500-1000	55,8	24,37	74,33
+250-500	68,03	29,72	44,62
+100-250	60,37	26,37	18,25
+60-100	27,22	11,89	6,36
+50-60	5,75	2,51	3,84
+25-50	6,85	2,99	0,85
-25	1,95	0,85	0,00
SUM	228,93	100	

Table 5-10: Result of screen analysis, LOI and density for fine fraction of mill product

Size (µm)	Mass (gr)	Mass (%)	Cum. Passing (%)	LOI (%)	Density (gr/cm³)
+60	0	0	100	---	---
+50-60	1,86	6,20	93,80	6,885	2,74
+25-50	6,17	20,57	73,23	6,99	2,82
-25	21,97	73,23	0,00	9,77	2,77
SUM	30	100,00		9,02	2,78

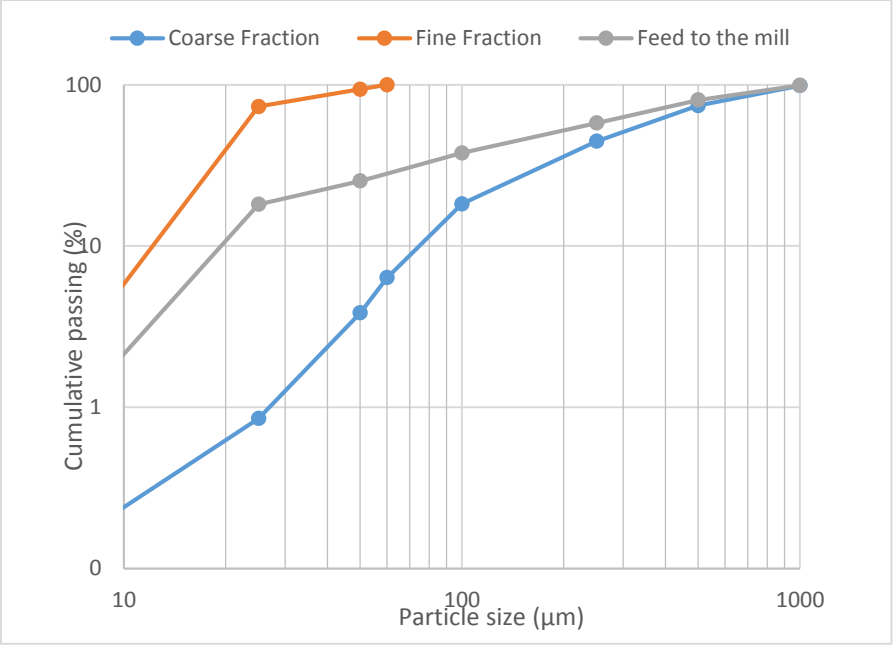

Fig. 5-3: Depiction of the result of screen analysis in the GGS plot

Regarding to the built partition curve, the size distribution of the stream between the mill and the classifier (the feed material to the air classifier as shown in fig. 5-2) and partition number (PN) for coarse and fine fractions, which is shown in fig. 5-4, are calculated in table 5-11.

Table 5-11: Calculated partition numbers for coarse and fine products of vertical roller mill

Size (µm)	Mass (%)	Coarse PN (%)	Fine PN (%)
+1000	0,98	100	0
+500-1000	18,56	100	0
+250-500	22,63	100	0
+100-250	20,08	100	0
+60-100	9,05	100	0
+50-60	3,39	56,40	43,60
+25-50	7,18	31,72	68,28
-25	18,11	3,58	96,42

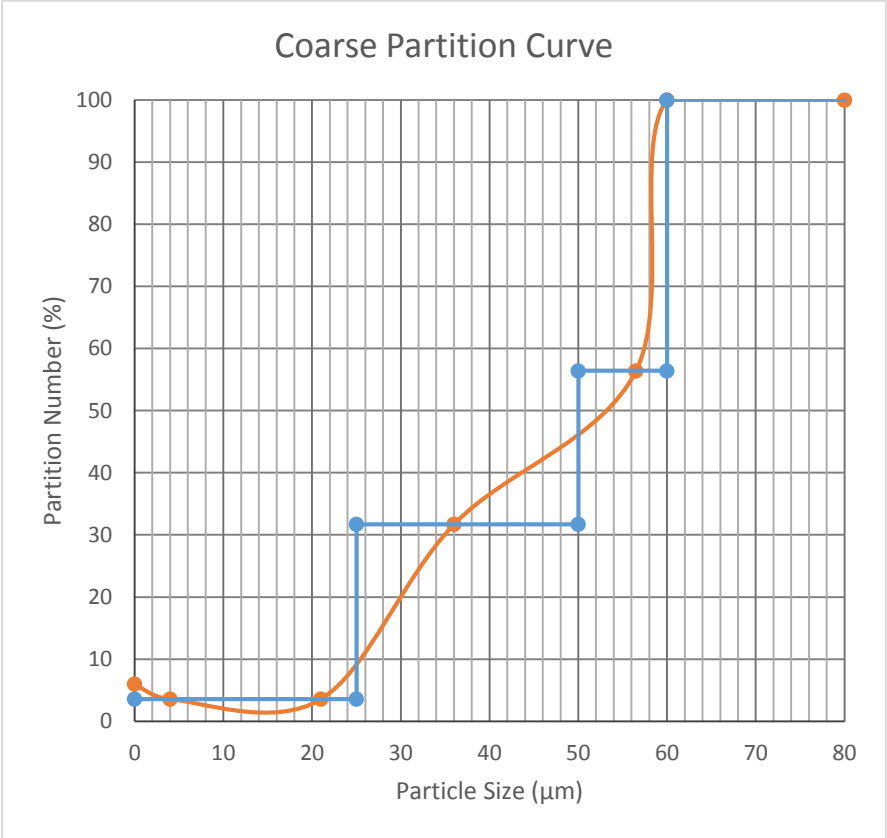

Fig. 5-4: VRM200. Partition curve of coarse material according to the setting of the mill and classifier given in tables 5-6 and 5-7

The partition curve values are also calculated from fig. 5-4 as shown in table 5-12.

Table 5-12: Characteristics figures derived from the partition curve fig. 5-4

	T 50	T 75	T 25	Cut Size	ep	Imperfection
Values	53 µm	58 µm	32 µm	53 µm	13 µm	0,24

$$ep = \frac{T_{75}-T_{25}}{2} \quad (32)$$

$$\text{Imperfection} = \frac{T_{75}-T_{25}}{2T_{50}} \quad (33)$$

T50 .....Tromp value

T75 .....particle size at 75% of partition number

T25 .....particle size at 75% of partition number

ep .....Écart probable

Imperfection .....the Écart probable related to the Tromp value

5-3- Bias measurement

Regarding to the wash water flowrate determination, an experiment was implemented to measure the bias rate against the wash water flowrate alteration. As it is discussed before, a zero or even slightly positive bias rate gives the best results regarding the concentrate grade and recovery. In contrast, the wash water flowrate must be big enough to penetrate into the cleaning zone.

The experiment was performed continuously in presence of the frother without solids. The flowrate of the overflow stream was measured with and without wash water stream.

The rate of overflow stream was measured at 0,5 cm^3/sec without wash water stream. Then, the experiment, at the same operation conditions, was

repeated in the presence of the wash water stream at 5,5 cm³/sec flowrate. The latter rate of overflow stream was obtained 2 cm³/sec. The summarized information of the measurement is shown in table 5-13.

Table 5-13: Results of bias measurement

Parameter	Value	Dimension
Feed flowrate	0,7	lit/min
Wash water flowrate	0,33	lit/min
Discharge flowrate	1,03	lit/min
Overflow rate without wash water	0,03	lit/min
Overflow rate with wash water	0,12	lit/min
Foam height	26,5	cm
Differential pressure	12,5	cm
Gas holdup	15.6	%
Compressed air pressure	0,3	bar
Bias rate	0,02	cm/sec

The bias rate in table 5-13 was calculated as follow:

Cell cross section area: $A_C = 52{,}04$ cm²

Overflow rate difference with and without water: $Q_w = 1{,}5$ cm³/sec

According to the superficial velocity formula, as mentioned in chapter two:

$$J_w = \frac{Q_w}{A_c} = 0{,}02\ cm/sec \qquad (34)$$

From now on, in the all flotation column experiments, the wash water flowrate is set at 0,33 lit/min up.

5-4- Flotation column test on talc ore

The test was carried out with the talc ore, the fine fraction product of the VRM200 with mentioned properties under the desired operation conditions as shown in table 5-14.

Table 5-14: Talc Column Flotation Operation Condition

Preparation of Suspension							
Conditioning Tank Vol.	Vol. Solid Content	Solid Density	Solid		Mass of Water	Pulp Density	Retention Time
			Vol.	Mass			
50 lit	4%	2,83 t/m³	0,002 m³	5,66 kg	48 kg	1,073 t/m³	210 sec

The column flotation experiments are aimed at a better understanding of the flotation cell behaviour and parameters. Therefore, some parameters like solid content of suspension and reagents dosage are not optimized. The adjusted values were obtained from literature and used only to proof the cell performance. After preparation of the feed pulp in the conditioning tank, the natural pH value of the slurry was measured at 8,25. The retention time was also controlled by adjustment of the feed flowrate according to the cell volume (9,5 lit). During this experiment, the feed and the wash water flowrates were manipulated at 2,7 lit/min and 0,33 lit/min, respectively. In order to keep the pulp level constant in the flotation cell, after filling up the cell till the desired level (about 10 centimetres above the feed port), the discharge flowrate was set up at 3,03 lit/min manually.

At this time the air valve was opened to inject the compressed air through the bubble generator at 0,3 bar pressure.

The only used additive as reagent, was frother (70 gram of MIBC per ton of dry solid). Therefore, the mass of the used frother according to the dry solid mass was calculated 0,4 gr.

Several series of samples from the foam and the discharge streams were taken during the experiment running time. In this experiment, each sample was taken for 10 sec. Because of being single operator, sampling was not performed, simultaneously. In each series of sampling, a complete cross section of the foam and the underflow streams was sampled. For the second and the third series of sampling, the mentioned sequence was repeated. From the obtained results by sampling, the mass balance table is formed in table 5-18. Table 5-15 shows the time schedule of the activities.

Table 5-15: Time schedule of talc ore experiment activities

Time schedule	
Mixer was started at	0 min
Reagent was added at	5 min
Feed valve was opened at	17 min
Air valve was opened at	26 min
Sampling 1 at	31 min
Sampling 2 at	36 min
Sampling 3 at	43 min

During this experiment, the compressed air pressure was adjusted at 0,3 bar and the differential pressure on gas holdup hoses was read at 9 cm. Therefore, the gas holdup, according to the equation 27, was calculated 11,2 %.

$$\text{Gas Holdup (\%)} = \frac{\Delta h}{H} * 100 \qquad (35)$$

Where:

"**Δ**h" is the difference level of pulp or liquid in gas holdup hoses and "H" is referred to the distance between to gas holdup outlets on the column cell body,

Table 5-16: Summarized features of talc ore column experiment

Parameter	Value	Unit
Difference height in gas holdup hose	9	cm
Gas holdup	11,2	%
Collection zone height	150	cm
Cleaning zone height	31,8	cm

The details of obtained samples are shown in table 5-17.

Table 5-17: Samplings data

Sample Name	Mass of Suspension (gr)	Mass of Dry solid (gr)
Sam. 1 Conc	205,67	23,59
Sam. 1 Tail	135,07	8,99
Sam. 2 Conc	142,05	19,28
Sam. 2 Tail	530,32	25,36
Sam. 3 Conc	355,95	38,92
Sam. 3 Tail	1070,68	74,44

Each single sample was washed at 25 (µm) to determine the flotation behaviour on the fine particles. Therefore, each sample was divided into two fractions, +25 µm and -25 µm. Afterwards, the samples were dried at 60

degree Celsius to avoid pyrite mineral oxidation. The mass balance table, which is shown in table 5-18, was developed according to the dry mass of samples, LOI and density values. The LOI and density values were gained as it described in section 5-1-1 & 5-1-2.

Table 5-18: Mass balance table for talc column flotation experiment

Sample	Mass (gr)	Mass recovery (%)	Fraction (µm)	Mass (gr)	Yield in sampling series (%)	Mass Recovery of Coarse (%)	Mass Recovery of Fine (%)	Density (gr/cm^3)	Density in product (gr/cm^3)	LOI (%)	Size related LOI recovery (%)	LOI in product (%)	LOI recovery (%)	(100-LOI) recovery (%)
Conc. S1	23,59	72,41	+25	9,05	27,78	78,96		2,85	2,86	5,33	66,48	6,02	93,98	73,66
			-25	14,54	44,63			2,88		6,45	53,45			
Tail. S1	8,99	27,59	+25	2,41	7,40	21,04		2,87	2,85	10,10	33,52	11,79	88,21	26,34
			-25	6,58	20,19			2,84		12,42	46,55			
Feed S1	32,58	100	+25	11,46		100,00		2,85	2,86	6,34	100,00	7,61	92,39	100,00
			-25	21,12				2,86		8,31	100,00			
Conc. S2	19,28	43,18996	+25	8,32	18,64	64,17		2,86	2,85	5,24	45,11	5,84	94,16	45,07
			-25	10,96	24,55			2,84		6,30	20,37			
Tail. S2	25,36	56,81004	+25	4,65	10,41	35,83		2,81	2,80	11,41	54,89	12,73	87,27	54,94
			-25	20,71	46,40			2,80		13,02	79,63			
Feed S2	44,64	100	+25	12,97		100,00		2,84	2,82	7,45	100,00	9,75	90,25	100,00
			-25	31,67				2,82		10,69	100,00			
Conc. S3	38,92	34,33	+25	19,70	17,38	49,00		2,83	2,84	5,24	40,43	6,01	93,99	35,69
			-25	19,22	16,95			2,84		6,79	15,71			
Tail. S3	74,44	65,67	+25	15,77	13,91	51,00		2,80	2,81	9,65	59,57	11,45	88,55	64,31
			-25	58,67	51,76			2,81		11,94	84,29			
Feed S3	113,36	100	+25	35,47		100,00		2,82	2,82	7,20	100,00	9,58	90,42	100,00
			-25	77,89				2,82		10,67	100,00			

The average recovery of LOI during the talc ore flotation column experiment was gained at 44,37%. As it is shown in table 5-18, the LOI values for concentrate and feed (table 5-18) are not constant. Therefore, the related recoveries are also different.

One of the reasons of the mentioned inconstancy in table 5-18 might be the instability in column cell operation conditions. Stable conditions in semi-batch processing systems as well as continuous systems, need time to establish. In other words, process stability is time dependent. In order to have more time to achieve stability in the lab column flotation process implementation of increased capacity of the conditioning tank is necessary.

In addition, operation conditions such as feed flowrate and compressed air flowrate during flotation experiments must be kept constant to reach stabilization. Alterations of slurry level in the conditioning tank, unsuitable shape and dimensions of impeller cause of changes in feed slurry flowrate. In order to keep the feed flowrate and underflow rate constant, it is necessary to use pumps of adjustable flowrate for both streams.

Because of absence of pumps, the conditioning tank and the mixing facilities are placed on the upper floor, as it is shown in fig. 3-12, to use the gravitational force for feed slurry discharge. This setup makes it impossible to control the conditioning tank and the column cell simultaneously for one operator.

The other reason for instable solid concentration, might be a pre-flotation and mineral segregation in the conditioning tank. Occurrence of this phenomena can change the characteristics of feed suspension during flotation. The relation of the dimensions of the impeller and the conditioning tank to have a suitable mixing environment during feeding is important to consider.

As it described before, the stream samplings could not performed simultaneously by the single operator. This fact can also be another reason for sampling errors rising.

Regarding to the mineralogical estimation of the flotation products, the carbon and sulphur content of products were measured by LECO apparatus and are illustrated in table 5-19. From these values, talc, pyrite and dolomite content of each product were also estimated.

Table 5-19: Estimated mineralogical composition of flotation products

Sample	Mass recovery (%)	Relative mass (%)	Carbon Content (%)	Sulphur Content (%)	Carbon Content in Product (%)	Sulphur Content in Product (%)	Carbon Recovery (%)	Sulphur Recovery (%)	Dolomite Content (%)	Pyrite Content (%)	Calculated LOI (%)	LOI- Cal. LOI (%)	Talc (%)	Dolomite (%)	Pyrite (%)	Residual (%)	related size talc recovery (%)	Talc recovery (%)
Conc. S1	72,41	78,96	0,15	0,04	0,35	0,07	31,79	56,03	2,719	0,134	0,63	4,71	99,14	1,00	0,07	0,00	81,39	96,04
		68,85	0,48	0,09							1,98	4,47	94,11	3,20	0,17	2,52	73,17	
Tail. S1	27,59	21,04	1,5	0,08	1,99	0,15	68,21	43,97	15,309	0,275	6,05	4,04	85,08	10,01	0,15	4,76	18,61	3,96
		31,15	2,17	0,17							8,79	3,62	76,26	14,48	0,32	8,94	26,83	
Feed S1	100	100,00	0,43	0,05	0,81	0,09	100,00	100,00	6,193	0,173	1,77	4,57	96,19	2,90	0,09	0,83	100,00	100,00
		100,00	1,01	0,11							4,10	4,21	88,55	6,71	0,22	4,52	100,00	
Conc. S2	43,18996	64,17	0,13	0,03	0,33	0,07	10,29	27,63	2,574	0,132	0,54	4,70	98,91	0,87	0,06	0,17	68,05	93,80
		34,61	0,49	0,10							2,02	4,27	89,93	3,27	0,19	6,62	37,79	
Tail. S2	56,81004	35,83	1,85	0,09	2,22	0,14	89,71	72,37	17,056	0,262	7,46	3,95	83,18	12,34	0,17	4,31	31,95	6,20
		65,39	2,30	0,15							9,30	3,72	78,34	15,34	0,28	6,03	62,21	
Feed S2	100	100,00	0,75	0,05	1,40	0,11	100,00	100,00	10,802	0,206	3,02	4,43	93,27	4,98	0,10	1,65	100,00	100,00
		100,00	1,67	0,13							6,78	3,91	82,35	11,16	0,25	6,23	100,00	
Conc. S3	34,33	55,54	0,15	0,04	0,35	0,07	9,33	19,65	2,711	0,131	0,63	4,62	97,22	1,00	0,07	1,70	56,05	95,87
		24,67	0,56	0,10							2,30	4,49	94,49	3,74	0,19	1,59	26,37	
Tail. S3	65,67	44,46	1,27	0,07	1,79	0,15	90,67	80,35	13,771	0,281	5,13	4,52	95,24	8,47	0,13	0,00	43,95	4,13
		75,33	1,93	0,17							7,83	4,11	86,43	12,88	0,32	0,38	73,63	
Feed S3	100	100,00	0,65	0,05	1,30	0,12	100,00	100,00	9,974	0,229	2,63	4,58	96,34	4,32	0,10	0,00	100,00	100,00
		100,00	1,59	0,15							6,47	4,20	88,42	10,62	0,29	0,68	100,00	

5-5- Mechanical flotation test on talc

A conventional batch flotation test has been carried out by a mechanical Denver flotation cell on the same characteristic talc ore sample of flotation column cell to compare the flotation results.

The volume solid content of the feed suspension was set at vol. 4%, to keep the pulp condition similarity to the mentioned column flotation test in section 5-4. General characteristics of the conventional flotation cell experiment are illustrated in table 5-20.

Table 5-20: Conventional Cell Experiment Characteristics

Density of solid	Vol. solid content	Mass of solid	Total vol. of cell	Mass of water	Density of suspension
2,82 gr/cm³	4%	180.48 gr	1,6 lit	1536 gr	1,073 gr/cm³

As described before, MIBC was used as the frother. The frother dosage was also selected at 70 gr/ton. Therefore, the frother mass needed was calculated at 0,012 gr of MIBC.

5-5-1- Test procedure

- After three minutes mixing of solid with water, the frother was added at t=0 to the pulp. The conditioning time for mixing the frother was two minutes. pH value was measured at 8,24.
- At t=2 min, the air valve was opened half. The foam was collected as first concentrate with duration of one minute (Conc. 1).
- At t=3:10 min, the second concentrate was taken with duration of four minutes (Conc. 2).

Fig. 5-5: Conventional flotation test on talc

- At t=7:15 min, the third concentrate was obtained. At this time, foam was not massive (Conc. 3).
- At t=8:43 min, the air valve was closed due to lack of foam and one more droplet of MIBC was added.
- At t=9:45, after one minute conditioning, the air valve was opened half again. At this stage, the froth seemed light (Conc. 4)
- At t=11:45 min the air valve was fully opened. At this stage the pH value was also measured again at 8,22. The bubbles were too small and not stable. The foam was light and there was no more load on the bubbles.
- At t= 13:44 the device was turned off.

The pH value of the residual suspension was determined at 8,23 at the end of the test. The duration of each product of the flotation experiments is given in table 5-21.

Table 5-21: Summarized Experiment Duration

Product	Conc. 1	Conc. 2	Conc. 3	Conc. 4	Residue
Duration	1 min	4 min	1:30 min	2 min	13:44 min

The products were screened wet at 25 µm mesh size, as described in section 5-4 for the column flotation. The LOI and density measurements were

included, in order to characterize the flotation products. The mass balance table is developed in table 5-22.

Table 5-22: Mass balance table for conventional cell experiment on talc

Sample	Mass (gr)	Float mass (%)	Washed wet at 25 (µm)	Mass (gr)	Mass in fraction (%)	Mass Recovery of Coarse and Fine (%)	Density (gr/cm^3)	Density in product (gr/cm^3)	LOI in Fraction (%)	LOI in product (%)	100- LOI (%)	Mass in Feed (%)	(100-LOI) Recovery (%)	(100-LOI) Recovery in Product (%)	Cum. Mass Recovery (%)
Conc. 1	55,69	31,492	+25	12,7	22,80	36,05	2,802	2,814	5,27	6,30	93,70	7,18	28,27	32,46	31,49
			-25	42,99	77,20	30,36	2,818		6,61			24,31	20,71		
Conc. 2	50,69	28,664	+25	9,39	18,52	26,65	2,814	2,811	5,16	6,03	93,97	5,31	20,44	29,63	60,16
			-25	41,3	81,48	29,16	2,81		6,23			23,35	18,76		
Conc. 3	7,91	4,473	+25	1,72	21,74	4,88	2,889	2,825	5,51	6,22	93,78	0,97	4,00	4,61	64,63
			-25	6,19	78,26	4,37	2,807		6,42			3,50	2,90		
Conc. 4	21,23	12,005	+25	5,93	27,93	16,83	2,818	2,815	5,20	6,31	93,69	3,35	13,02	12,37	76,63
			-25	15,3	72,07	10,80	2,814		6,75			8,65	7,52		
Tail	41,32	23,366	+25	5,49	13,29	15,58	2,695	2,744	14,79	18,60	81,40	3,10	34,28	20,92	100,00
			-25	35,83	86,71	25,30	2,752		19,19			20,26	50,11		
Feed	176,8	100	+25	35,23	19,92	100,00	2,795	2,798	6,73	9,10	90,90				
			-25	141,61	80,08	100,00	2,798		9,69						

5-6- Graphite sample

The graphite sample was raw ground ore and obtained from Kaiserberg graphite mine near to Leoben. From the mineralogical aspect, the gangue minerals content are mostly; quartz, feldspar, tourmaline, mica, pyrite, amphibolite, chlorite, augite, sericite. The average carbon and moisture content of the raw material sample were measured at 54,4% and less than 0,1%, respectively.

The results of the particle size distribution by air jet screening is shown in table5-23.

Table 5-23: Particle Size Distribution via Air Jet

Fraction (µm)	Mass (gr)	Mass (%)	Cum. Passing (%)
+100	0	0,00	100
+71-100	0,62	4,13	95,87
+50-71	1,64	10,93	84,93
+40-50	1,15	7,67	77,27
+25-40	2,4	16,00	61,27
-25	9,19	61,27	0,00
SUM	15		

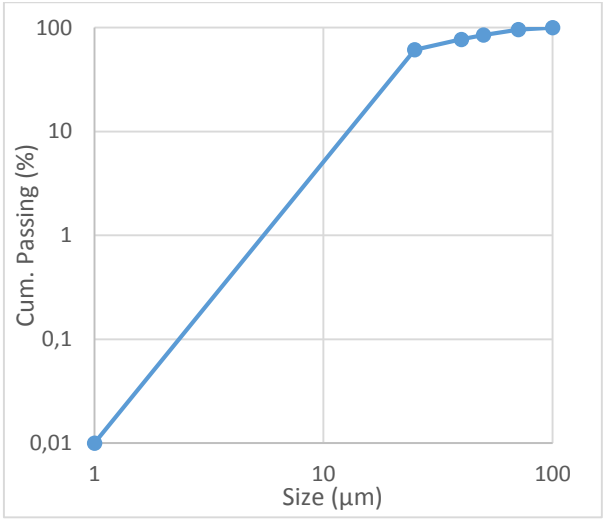

Fig. 5-6: Depiction of graphite screen analysis result in GGS plot

Table 5-24 is also shown the carbon concentration of the size fraction.

Table 5-24: Carbon Content in Size Classes

Fraction (µm)	Mass (%)	Carbon Content (%)	Carbon Recovery (%)
+100	0	0	0,00
+71-100	4,13	63,53	4,83
+50-71	10,93	58,45	11,75
+40-50	7,67	55,13	7,78
+25-40	16	53,66	15,79
-25	61,27	53,12	59,86
SUM	100	54,37	100

5-7- First graphite flotation test

The experiment was implemented by the column flotation cell on the graphite ore sample with the properties mentioned in section 5-6. The operation conditions are illustrated in table 5-25.

Table 5-25: Graphite Sample Operation Condition

Preparation of Suspension							
Conditioning Tank Vol.	Vol. Solid Content	Solid Densit	Solid		Mass of	Pulp Densit	Retention Time (sec)
			Vol.	Mass			
50 lit	4%	2,47 gr/cm³	0,002 m³	4950 gr	4800 gr	1,059 gr/cm³	160

The feed and wash water flowrates were 3,5 lit/min and 0,33 lit/min, respectively. Therefore, the underflow discharge to keep the pulp level constant was 3.83 lit/min.

680 gr/ton was selected as reagents dosage for both collector and frother. The time table and sequence of activities are shown in table 5-26.

Table 5-26: Sequence of Activities

Time schedule		
Mixer was started at		0 min
Reagents added at	Collector	5 min
	Frother	8 min
Feed valve was opened at		13 min
Air valve was opened at		17 min
Sampling 1 at		19 min
Sampling 2 at		24 min
Sampling 3 at		27 min

Details of the samplings along the experiment with the graphite ore are shown in table 5-27. The sampling duration was 10 seconds and constant for all samples.

Table 5-27: Sampling details of first graphite experiment

Sample Name	Mass of Suspension (gr)	Mass of Dry solid (gr)
Sam. 1 Conc	103,26	10,83
Sam. 1 Tail	180,24	2,91
Sam. 2 Conc	76,84	8,46
Sam. 2 Tail	127,06	16,47
Sam. 3 Conc	198,67	17,49
Sam. 3 Tail	383,08	21,08

The experiment was run at slightly more than 0,3 bar compressed air pressure. The gas holdup height difference was measured at 10,5 cm in average, which led to 13,1 % gas holdup.

Table 5-28: Measured parameters of experiment

Parameter	Value	Unit
Difference height in gas holdup hose	10,5	cm
Gas holdup	13,1	%
Collection zone height	152,5	cm
Cleaning zone height	29,3	cm
Sampling duration	10	sec
Carrying capacity rate	0,023	gr/sec/cm²

In this experiment, due to short sampling time, the dry mass of the samples was not sufficient for screening at 25 µm. Therefore, the mass balance was formed by the dry mass of the samples, without wet screening, and is shown in table 5-29.

Table 5-29: Mass balance table of first graphite column flotation experiment

Samples	Dry Solid Mass (gr)	Mass (%)	Ash Content (%)	Carbon Content (%)	Density (gr/cm³)	Carbon Recovery (%)
Conc. S1	10,83	78,82	23,90	76,10	2,32	90,53
Tail S1	2,91	21,18	70,37	29,63	2,64	9,47
Feed S1	13,74	100,00	33,74	66,26	2,39	100,00
Conc. S2	8,46	33,94	21,34	78,66	2,30	43,63
Tail S2	16,47	66,06	47,80	52,20	2,45	56,37
Feed S2	24,93	100,00	38,82	61,18	2,40	100,00
Conc. S3	17,49	45,35	31,41	68,59	2,34	57,77
Tail S3	21,08	54,65	58,40	41,60	2,52	42,23
Feed S3	38,57	100,00	46,16	53,84	2,44	100,00

5-8- Second graphite flotation test

The operation conditions of the flotation test are given in table 5-30. With regard to trace flotation behaviour for the fraction -25 µm and +25 µm, it is assumed that there is no valid solid is obtained during short sampling duration. In order to investigate the feed pulp rheology properties on the gas hold up, in the second graphite ore experiment, the feed suspension solid content was decreased from 4% in the first column test to 2%. The solid content was changed to investigate the effect of the feed suspension density on the gas hold up.

Table 5-30: Graphite Column Experiment Operation Condition

Preparation of Suspension							
Conditioning Tank Vol.	Vol. Solid Content	Solid Density	Solid		Mass of Water	Pulp Density	Retention Time (sec)
			Vol.	Mass			
50 lit	2%	2,47 t/m³	0,001 m³	2.5 kg	49 kg	1,029 t/m³	240

The column operation settings such as pulp level, wash water flowrate, sequence of the test implementation and the cell control procedure were kept the same as mentioned before for the talc ore and the first graphite ore flotation test in sections 5-4 and 5-7. The reagents added to floathe the graphite, were diesel and MIBC as collector and frother, respectively. The collector and frother were added into the conditioning tank with three minutes time difference.

The feed and wash water flowrates were 2,4 lit/min and 0,33 lit/min. Therefore, the underflow discharge was 2,73 lit/min to keep the constant pulp level in the column cell. The time schedule of activities are shown in table 5-31.

Table 5-31: Time schedule of graphite experiment

Time schedule		
Mixer is started at		0 min
Reagents added at	Collector	3 min
	Frother	6 min
Feed valve is opened at		9 min
Air valve opened at		14 min
Sampling 1 at		18 min
Sampling 2 at		24 min
Sampling 3 at		32 min

The details of the obtained samples are shown in table 5-32. The sampling duration is 40 sec.

Table 5-32: Sampling Details of Graphite Experiment

Sample Name	Mass of Suspension (gr)	Mass of Dry solid (gr)
Sam. 1 Conc	487,61	55,44
Sam. 1 Tail	425,74	3,84
Sam. 2 Conc	802,7	24,6
Sam. 2 Tail	1250,07	38,64
Sam. 3 Conc	952,24	62,28
Sam. 3 Tail	1700,5	39,76

During this experiment, the injected compressed air pressure and the gas holdup difference height were read at 0,3 bar and 11,5 cm, respectively.

Table 5-33: Charactristics of column experiment on graphite

Parameter	Value	Unit
Difference height in gas holdup hose	11,5	cm
Gas holdup	14,4	%
Collection zone height (h_c)	154,5	cm
Cleaning zone height	27,5	cm
Interstitial velocity (U= h_c/τ)	0,85	cm/sec
Slurry superficial velocity (J_{sl})	0,86	cm/sec
Axial mixing coefficient E	29,04	cm²/sec

In table 5-33, the axial mixing coefficient (E) is calculated according to the equations (28) and (29):

$$6_r{}^2 = 2N_d - 2N_d^2\left[1 - e^{\frac{-1}{N_d}}\right] \quad (36)$$

$$E = N_d.u.h_c \quad (37)$$

Where:

N_d ..... Dispersion number

The dispersion number and the axial mixing coefficient are calculated as 0,22127 and 29,04 cm²/sec, respectively.

Table5-34: Mass balance table for the second graphite ore test

Samples	Mass of dry solid (gr)	Yield in sampling series (%)	Density of dry products (gr/cm³)	Fraction (µm)	Mass (gr)	Mass (%)	Mass Recovery of Coarse (%)	Mass Recovery of Fine (%)	Ash content (%)	Size related ash recovery (%)	Ash content in product (%)	Carbon content (%)	Density (gr/cm³)	Carbon Recovery (%)
Conc. S1	55,44	93,53	2,31	+25	33,33	56,23	97,10		21,71	91,28	25,88	74,12	2,27	97,79
				-25	22,11	37,30		88,61	32,18	76,24			2,36	
Tail S1	3,84	6,47	2,68	+25	1,00	1,68	2,90		69,47	8,72	75,80	24,20	2,68	2,21
				-25	2,84	4,79		11,39	78,02	23,76			2,68	
Feed Sam.1	59,28	100,00	2,33	+25	34,32	57,90	100,00		23,09	100,00	29,11	70,89	2,28	100,00
				-25	24,95	42,10		100,00	37,40	100,00			2,39	
Conc. S2	24,60	38,90	2,56	+25	16,86	26,67	58,18		29,50	42,54	33,71	66,29	2,31	49,97
				-25	7,73	12,23		22,58	42,89	17,55			3,11	
Tail S2	38,64	61,10	2,52	+25	12,12	19,17	41,82		55,44	57,46	57,74	42,26	2,48	50,03
				-25	26,51	41,93		77,42	58,79	82,45			2,53	
Feed Sam. 2	63,23	100,00	2,53	+25	28,99	45,84	100,00		40,35	100,00	48,39	51,61	2,38	100,00
				-25	34,25	54,16		100,00	55,20	100,00			2,66	
Conc. S3	62,28	61,03	2,33	+25	21,80	21,36	65,82		23,50	39,56	30,79	69,21	2,28	78,83
				-25	40,50	39,69		58,75	34,71	40,87			2,36	
Tail S3	39,76	38,97	2,61	+25	11,32	11,09	34,18		69,14	60,44	70,85	29,15	2,56	21,17
				-25	28,44	27,87		41,25	71,53	59,13			2,63	
Feed Sam. 3	102,04	100,00	2,44	+25	33,12	32,46	100,00		39,09	100,00	46,39	53,61	2,37	100,00
				-25	68,94	67,56		100,00	49,90	100,00			2,47	

5-8-1- Residence time distribution determination

During the second column flotation test with the graphite ore, the residence time was also measured by injection of a saturated salt solution as an impulse tracer into the column. The solution was prepared by the magnetic impeller at room temperature and injected with a syringe near to the feed port into the cell. At the time of injection (t=0), the first sample was taken from the underflow discharge. 26 more time dependent samples were also obtained from the underflow of the cell with 7 seconds time interval between samplings. An average, the sampling duration was also 7 seconds. By means of the conductivity value, the concentration of tracer was followed in the samples. The conductivity measurement apparatus was calibrated with 0,01 mol/lit potassium chloride solution, according to the device manual.

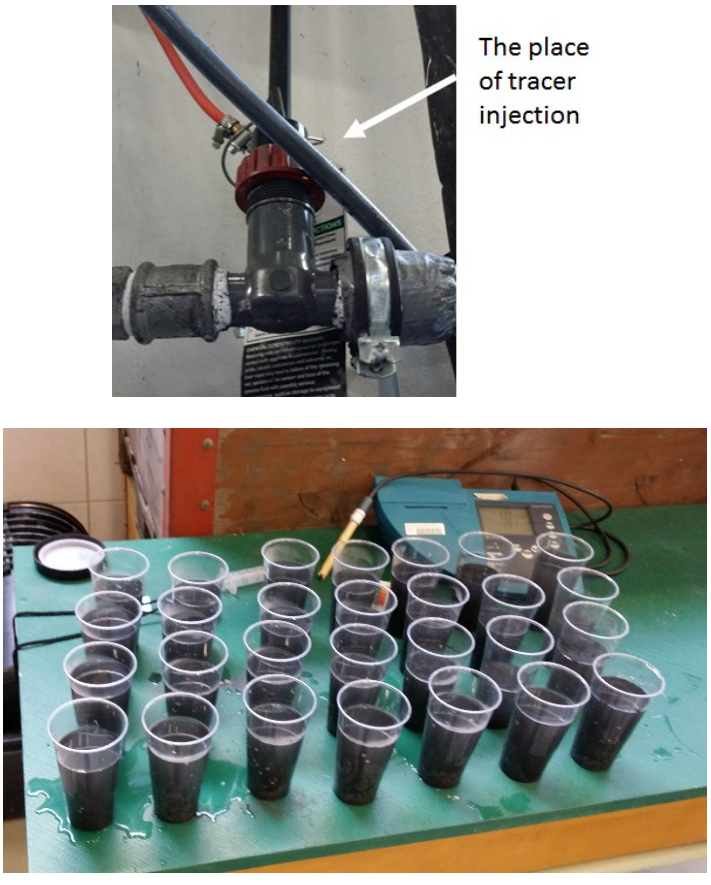

Fig. 5-7: Obtained samples for residence time distribution determination

Residence time distribution diagram and the results of the residence time are shown in table 5-35 and fig. 5-8.

Table 5-35: Sampling information for residence time distribution determination

Sequence (j)	Time (sec)	Conductivity (µS/cm)	$t_j * C_j * \Delta t_j$	$C_j * \Delta t_j$	$(t_j - \tau_j)^2 * C_j * \Delta t_j$
1	0	363	0	2541	82669333,3
2	14	363	35574	2541	70334239,6
3	28	365	71540	2555	59320260,5
4	42	370	108780	2590	49590466,4
5	56	390	152880	2730	42228932,2
6	70	395	193550	2765	33683364
7	84	397	233436	2779	25810305,9
8	98	398	273028	2786	18903563,5
9	112	396	310464	2772	12958472,9
10	126	393	346626	2751	8132915,82
11	140	388	380240	2716	4426873,61
12	154	385	415030	2695	1874370,14
13	168	383	450408	2681	410392,031
14	182	381	485394	2667	7065,8183
15	196	378	518616	2646	646217,931
16	210	375	551250	2625	2304223,89
17	224	372	583296	2604	4956387,69
18	238	372	619752	2604	8647753,29
19	252	370	652680	2590	13288059,5
20	266	373	694526	2611	19144113,2
21	280	366	717360	2562	25429579,7
22	294	366	753228	2562	33078623,2
23	308	365	786940	2555	41617948,8
24	322	364	820456	2548	51108804,4
25	336	363	853776	2541	61542958
26	350	364	891800	2548	73315007,2
27	364	363	924924	2541	85680298,7
SUM			12825554	71106	831110531

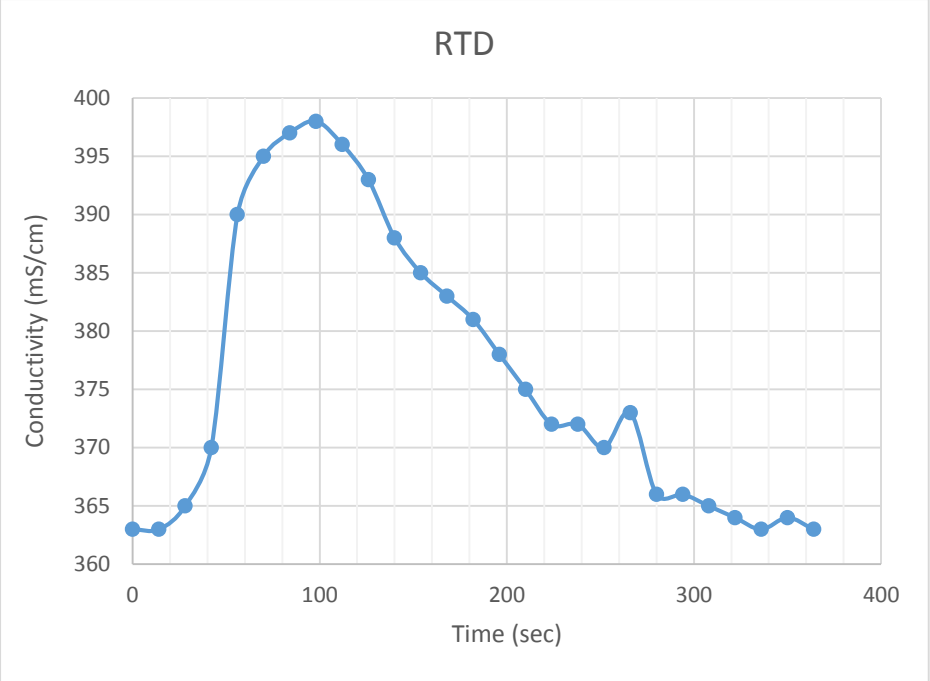

Fig. 5-8: Residence time distribution diagram

The residence time, variance and relative variance were calculated according to the equations in section 2-1-16. The results are shown in table 5-36.

Table 5-36: Calculated residence time, variance and relative variance

τ	6^2	$6_r{}^2$
180 sec	11688 sec	0,36

5-8-2- Pulp density and gas holdup correlation

As discussed before, the gas holdup is one of the most important parameters which has a direct effect on the froth carrying capacity and the process performance. The gas holdup parameter depends on a variety of parameters such as the sparger type, the gas consumption, the bubble size, machine and operation condition and etc.

Of course, all the parameters affecting the gas holdup are of interest, however it needs more measurement facilities to keep stable conditions during the process. In this investigation, only the effect of the feed slurry density on the gas holdup is determined and shown in table 5-37. It is important to mention that the effect of narrow variations in some variables, such as the feed flowrate, the overflow rate or compressed air pressure alterations, are not considered in this investigation.

Table 5-37: Measured feed slurry density against gas holdup

Slurry Density (gr/cm^3)	Gas holdup (%)
1	15,6
1,073	11,2
1,059	13,1
1,029	14,4

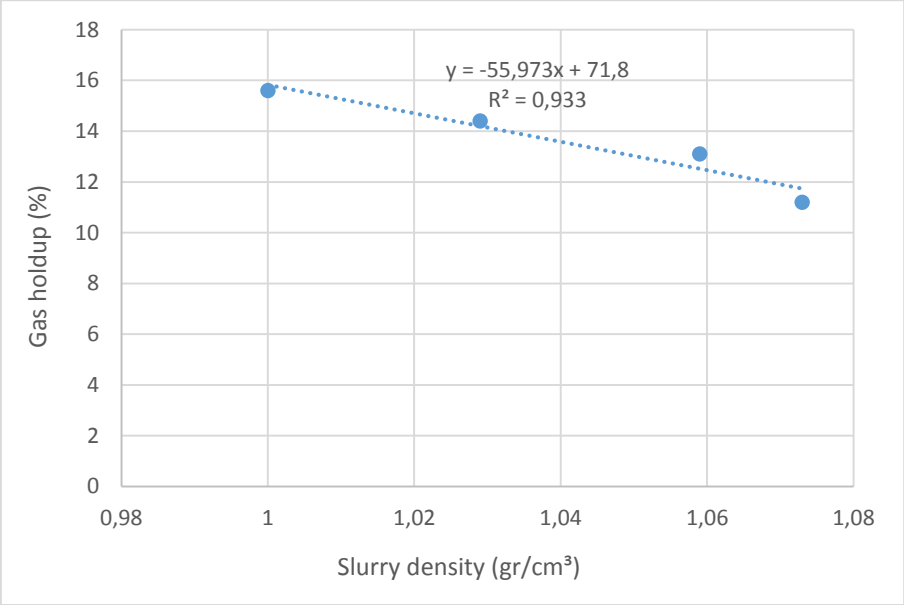

Fig. 5-9: Correlation between gas holdup and slurry density

As it has been illustrated in fig 5-9, an equation is developed to estimate the gas holdup value. The correlation coefficient is also determined as R^2=0,93.

5-9- Discussion

As it is mentioned in talc sample ore description (section 5-2), the flotation feed LOI was measured at 9,02%. In table 5-18, LOI values of the flotation feed, obtained from the back calculation of the column flotation products, vary from 7,6 to 9,75 and 9,58 for first, second and third series of sampling, respectively. A comparison of the measured and the calculated results in table 5-18 shows that the third series of sampling has the nearest results to the nominal feed properties. Moreover, the grade of products and LOI recovery of each series of samplings fluctuate. The mentioned inconstancies, could be the reason for the instability in the column cell operation conditions. In semi-batch processing systems as well as continuous systems, the process stabilization is time dependent. In addition, the manual settings adjustment of the air, the input and the output slurry flowrates are time consuming and alter the solid content of the prepared feed suspension. Therefore, the amount of feed suspension to perform a stable flotation test should be increased.

In order to achieve more stable conditions, the application of pumps for adjustment of input and output flowrates can be a solution to keep a constant level of suspension in the cell.

Furthermore, the level of feed suspension in the conditioning tank is constantly decreasing during flotation process implementation. The changes of the suspension level in the conditioning tank, cause a differential pressure and thus, suspension velocity alterations. This suspension velocity changes affected the feed pulp flowrate caused instability in the operation conditions. In the current setup, the feed pulp flowrate decreases with the flotation duration.

The other reason for the inconstancy in column cell performance might be the effect of a pre-flotation and mineral segregation in the conditioning tank. Occurrence of this phenomena can change the characteristics of the feed suspension during flotation. The dimension ratio of the impeller and the conditioning tank in order to provide an improved mixing environment during feeding is important to consider.

In the mechanical flotation test on the alc ore, which was performed at the same operation conditions and same feed material of column flotation test as the column test, the LOI of the concentrate was obtained at 6,17% with a concentrate mass recovery at 60,16%. The comparison of the column and conventional flotation results show, slightly higher concentrate purity of column test than the conventional apparatus, although the obtained yield in column was less than in the conventional cell.

According to the obtained results of the tracer experiment within the saturated salt solution, the mean residence time is obtained at 180 second. At the beginning of the experiment, the feed flowrate was set at 2,4 lit/min. The calculated mean residence time from the tracer experiment is in good agreement with the retention time from plug flow

6- Suggestion for improvement

The suggestions that are recommendations for improvements in this section are based on the experience obtained during the current tests. The aim of this work study was the construction of the simplest generation of a flotation column cell. To increase experiments accuracy, the implementation of more facilities is necessary. As it has been shown in mass balance tables, a fluctuation is obvious in the products grade and recovery. By slurry discharging from conditioning tank, which is placed on the upper floor, the feed flowrate is changed during flotation test due to pressure alteration. In addition, pulp level adjustment in the column is carried out by manual feed and discharge valves manipulation, which is not easy to perform and accurate. It is also time consuming.

a) To achieve stable operation conditions for a semi-batch processing system, a constant level of different parameters such as feed slurry flowrate is needed. The flowrate of input streams and output stream must be equal to have a constant level of suspension in the column cell. It is recommended, as applied in commercial laboratory column flotation cells, to apply two peristaltic pumps with the same properties for feed and underflow streams. The most common used pump for laboratory column cells is the peristaltic pump. They are more comfortable for low flowrates adjustments.

b) Feed pulp conditioning has also an important effect on the column performance from two points of view. In some cases, due to high density difference of minerals, mineral segregation during conditioning may occur. The impeller design and rotational speed needs more investigation to improvement. Another points to mention concern the conditioning tank volume. A continuous experiment needs more time to reach to stable conditions. Manual settings are also time consuming and waste the prepared feed suspension before flotation commence. Therefore, the conditioning tank must have the capacity for process stabilization.

c) Air flowmeter to measure air volume consumption during the experiment is of advantage for further flotation parameters evaluation. This measurement leads to calculate more parameters of the column such as gas superficial velocity and carrying capacity of bubbles. These equipment must be sensible enough for a laboratory device settings.

d) As it is observed by the author of this investigation work, narrow alterations of compressed air pressure influence the bubble rise velocity and flotation performance significantly. The range of the compressed air alterations depend on the pulp rheology properties, suspension solid content and pulp density.

e) The wash water flowrate and the bias rate influenced on the bubble carrying capacity and the concentrate grade. It is recommended to investigate optimum bias rate and wash water flowrate.

f) The kinetics of flotation is an effective parameter to achieve to the stable conditions.

References:

1. M. C. Fuerstenau, G. Jameson, R. H. Yoon, Froth Flotation; A Century of Innovation, SME, pp: 69-71.

2. J. B. Yianatos, Column Flotation Modelling and Technology, Chemical Engineering Department, University of Santa Maria, Valparaiso, Chile, pp: 1-31

3. A, Mular , D.N. Halbe, D.J. Barratt, Mineral Processing Plant, Design, Practice and Control, Vol. I, SME, 2002, pp: 1097-1140.

4. S. Chander, R. R. Klimpel, Advances in Coal and Mineral Processing Using flotation, Society for Mining, Metallurgy and Exploration Inc., 1989, pp: 347-355

5. http://www. metso.com /products/separation/microcell-high-recovery-flotation-columns/

6. S.K. Biswal, Flotation Column: A Novel Technique in Mineral Processing.

7. R. R. Klimpel, (1995), "The influence of the frother structure on Industrial Coal Flotation", High- Efficiency Coal Preparation (Kawatra, ed.), Society for Mining, Metallurgy and Exploration, Littleton, CO, pp. 141-151

8. J.B. Rubinstein, Column Flotation Processes, Design and Practices. Gordon and Breach Science Publishers, Institute of Solid Fuels Preparation, Moscow, Russia, 1995, pp: 67-74,103-107, 181-190, 273-276.

9. J.B. Yianatos, J.A. Finch and A.R. Lapante, Hold up profile and bubble size determination of flotation column frothers, Canadian Metall. Quarterly, 1986,25(1).

10. J.T. Furey, Rougher Column Flotation of Gold Tellurides. CMP Proc. 22nd Annual Meeting, 1990.

11. R. Espinoza- Gomez and N.W. Jamson, Technical Experience with Conventional Columns at Mount Isa Mines Limited, Column 91, Proceeding of an International Conference on Column Flotation, (G.A. Agar, B.J. Huls, and D.B. Hyma, eds.), Sudbury, Ontario, Canada, June1991, pp: 511-524.

12. R.D. Villar, M. Gregoire and A. Pomerleau, Mineral Engineering, Vol. 12, Pergamon, 1991, No. 3, p. 291-308.

13. F.J. Tavera, R. Escudero, J. A. Finch, Gas Holdup in Flotation Column; Laboratory Measurements, International Journal of Mineral Processing, 2001, p. 23-40

14. M. Xu, Sparger Study in Flotation Columns, Master Dissertation, Department of Mining and Metallurgical Engineering, McGill University, 1987, pp: 4-28, 44-56,

15. J.B. Yianatos, A.R. Levy, Estimation of Gas Holdup, Diameter and Apparent Density of Mineralized Bubbles in Industrial Flotation Columns, Department of Chemical Engineering, University Santa Maria, Valparaiso, Chile.

16. J.A. Finch and G.S. Dobby, Column Flotation, Pergamon press, 1990.

17. J.A. Finch, Column Flotation: A Selected Review- Part IV: Novel Flotation Devices, Mineral Engineering, pergamon, 1995, Vol. 8, No. 6, pp.: 587-602.

18. Y.T, Shah,. et al; Design parameters estimations for bubble column reactors, 1982, AIChE J. vo1.28 No.3, p.: 353- 363,

19. D.A. Wheeler, Column Flotation- the original column, 87th Annual General Meeting, CIM Vancouver, 1985, Aug.

20. G.B. Wallis, One Dimensional Two-phase flow, McGraw-Hill, New York, AlChE Journal, 1969, Chapter. 9.

21. J.F. Richardson and W.N. Zaki, Sedimentation and fluidisation: part I, Department of Chemical Engineering, Imperial College, London, 1954, Vol. 32, pp: 32-35,
22. D. Bhaga, Master Thesis, McGill University, Montreal, Canada, 1970.

23. G.J. Jameson, S. Nam and M. Moo Young, Physical factors affecting recovery rates in flotation, Mineral Science Engineering Journal, 1977, Vol. 9, No. 3.

24. S.R.S. Sastri, Technical Note: Carrying Capacity in Flotation Columns, Pergamon, Mineral Engineering, 1996, Vol. 9, No. 4, p. 465-468.

25. M. Falutsu, and G.S. Dobby, Froth Performance in Commercial Sized Flotation Columns, Mineral Engineering, Vol. 5, 1992, 5(10-12), pp: 1207-1223.

26. S.A. Flynn and E.T. Woodburn, Development of a Froth Model for Fine Particles Beneficiation by Flotation, 1987, Transaction of Institution of Mining and Metallurgy, 1987, Section C, 96, Dec., C96, C191 and C191-C198.

27. R.M. Yoon, M.J. Mankosa, G.H. Luttrell, Design and Scale up Criteria for Column Flotation, XVIII International Mineral Processing Congress, Aus., IMM Sydney, Australia, 1993, 785.

28. R. Espinonza- Gomez, J.A. Finch, J.B. Yianatos, G.S. Dobby, Flotation Column Carrying Capacity: particle Size and Density Effect, 1988, Mineral Engineering, Vol. 1, pp: 77-79.

29. R. Espinonza- Gomez, J.A. Finch, J.B. Yianatos, Carrying Capacity Limitations in Flotation Columns, In: K.V.S Sastry (ed.), Column Flotation-88, Proceeding of International Symposium on Column Flotation, Soc. of Mining Engineering (SME), Littleton, CO, 1988, pp:143-148.

30. R. Perez Garibay, A.P.M. Gallegos, S A. Uribe, A F. Nava, Effect of Collection Zone Height and Operating Variables on Recovery of Overload Flotation Columns, Mineral Engineering Journal, 2002, 15, p.: 325-331

31. K.S. Kawatra, T.C. Eisele, Flotation Column Design for Coal Phosphate Processing. In: Proceeding of IX Congreso Internacional de Metalurgia Extrativa., Universidad de Sonora, Mexico, 1999, p.: 43-66.

32. I.I. Maksimov, A.D. Borkin, M.F. Emelyanov, The Use of Column Flotation machines for Cleaning Operations in Concentrating non-ferrous Ores. In: Proceeding of XVII International Miner Processing Congress, Dresden, FRG, Vol. 2, p.: 273-281.

33. A.Roberts, Mineral Processing, Proceeding of the Sixth International Congress, Cannes, 1963, May 26- June 2, pp: 595-601

34. D. Lelinski, J. Allen, L. Redden, A. Weber, Analysis of the residence time distribution in large flotation machines, Mineral Engineering, 15, 2002, pp: 499-505

35. B. Oteyaka, H. Soto, Air Velocity and Turbulence Effects in Flotation, Pres. 33rd , Annual Conference of Metallurgists, The Metallurgical Society of CIM, Toronto, Aug. 1994, pp: 20-25.

36. Z.A. Zhou, Z. Xu, J.A. Finch, Minimum Recovery Zone Height Requirements in Flotation Columns from Particle- Bubble Collision Analysis, Submitted to Mineral Eng., Vol. 104, 1995, pp: 102-106.

37. M.K. Ityokumbul, Design and Scale up issues in Column Flotation, Innovations of Mineral Processing, Acme Printers, Sudbury, Canada, 1994, pp: 187-200.

38. J.B. Yianatos, J.A. Finch, G.S.Dobby and A.R. Lapante, Effect of Column Height on Flotation Column Performance, Mineral and Metallurgical Process, 1988, pp: 11-14.

39. R. del Villar, A. Desbiens, J.F. Huard, J. Bouchard, F.O. Verret, An Experimental Set-up for the Study of Flotation Column Optimization, University of Laval, Quebec, Canada.

40. G.G. Roy, R. Shekher, S.P. Mehrotra, Particle Suspension in (air agitated) Pachuca Tanks, Metallurgical and Material Transactions, 1998, 29 (B), 339-349.

41. J.A. Finch, J. Xiao, C. Hardie, C.O. Gomez, Gas Dispersion Properties: Bubble Surface Area Flux and Gas Holdup, Mineral Eng. Journal, Vol. 13, No. 4, 2000, pp: 365-372.

42. S. Banisi, J.A. Finch, Technical note: Reconciliation of Bubble Size Estimation Methods using Drift Flux Analysis, Mineral Engineering, 1994, 7(12), pp: 1555-1559

43. R. J. King, Mineral Explained, No. 2, Graphite, Blackwell Publishing, Geology today, Vol. 22, 2006, pp: 71- 77.

44. C.A. Landis, Contrib. Mineral. Petrol., 1971, 30, pp: 34-45

45. A. Yehia, M.L. AL-Wakeeel, Talc separation from talc carbonat ore to be suitable for different industrial applications, Mineral Engineering, 2000, pp: 111-116.

46. W. Perruk, Applied Mineralogy in the Mining Industry, Elsevier, 2000, pp: 190-194

47. M. Khraisheh, C. Holland, C. Creany, P. Harris, L. Parolis, Effect of molecular weight and concentration of the adsorption of CMC onto talc at different ionic strengths, International Journal of Mineral Processing, 2005, pp: 197-206

48. G.Y. Boghdady, M.M. Ahmed, G.A. Ibrahim, M.M.A. Hassan, Petrographical and geochemical characterisation of some Egyptian talc samples for possible industrial applications, Journal of Engineering Science, 2005, p.: 1001-1011.

49. http://www.leco.com

50. A. Böhm, Internal Report, Montan University of Leoben, Austria.

Appendix 1: Foam Launder

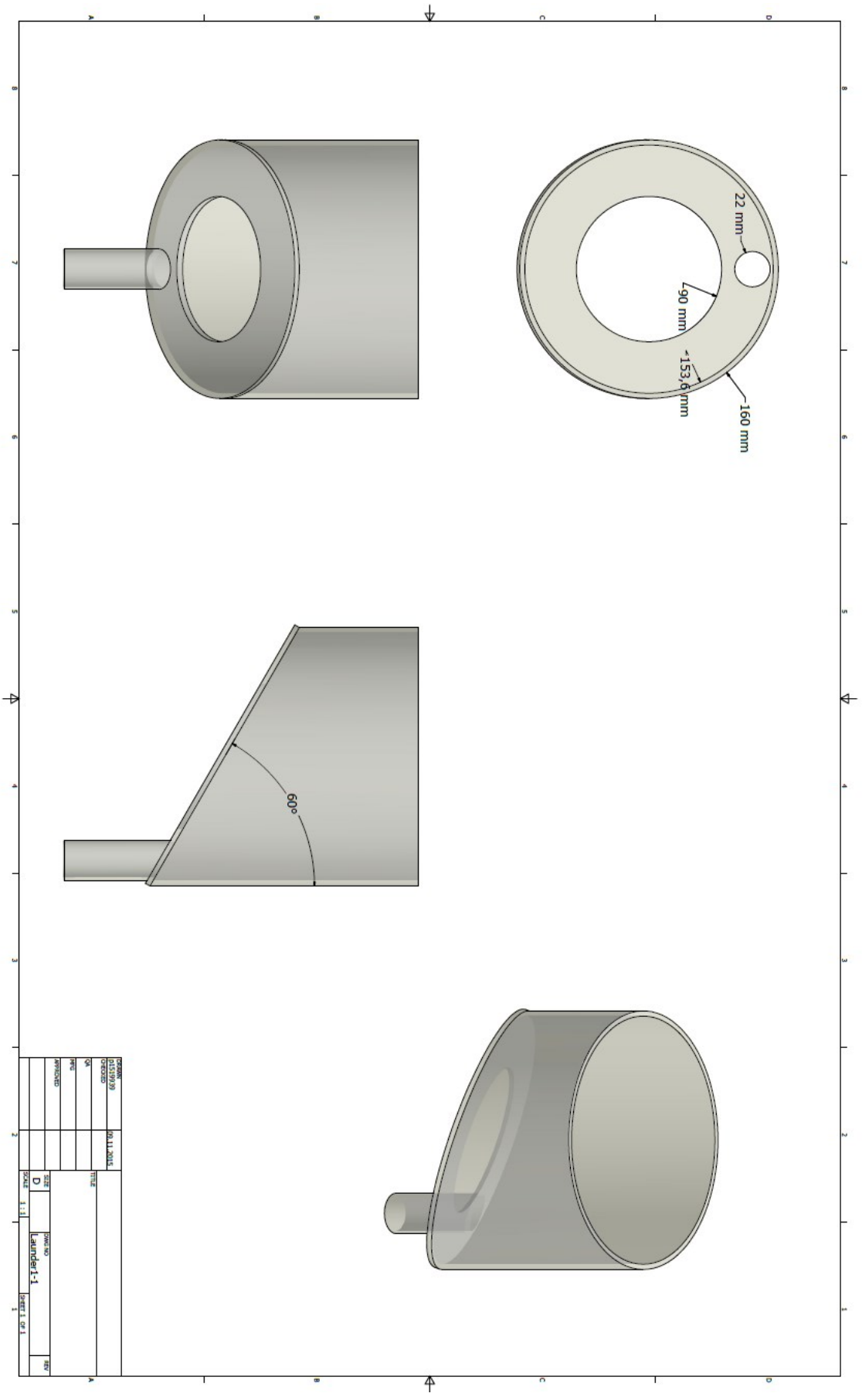

Appendix 2: Main Upper Part

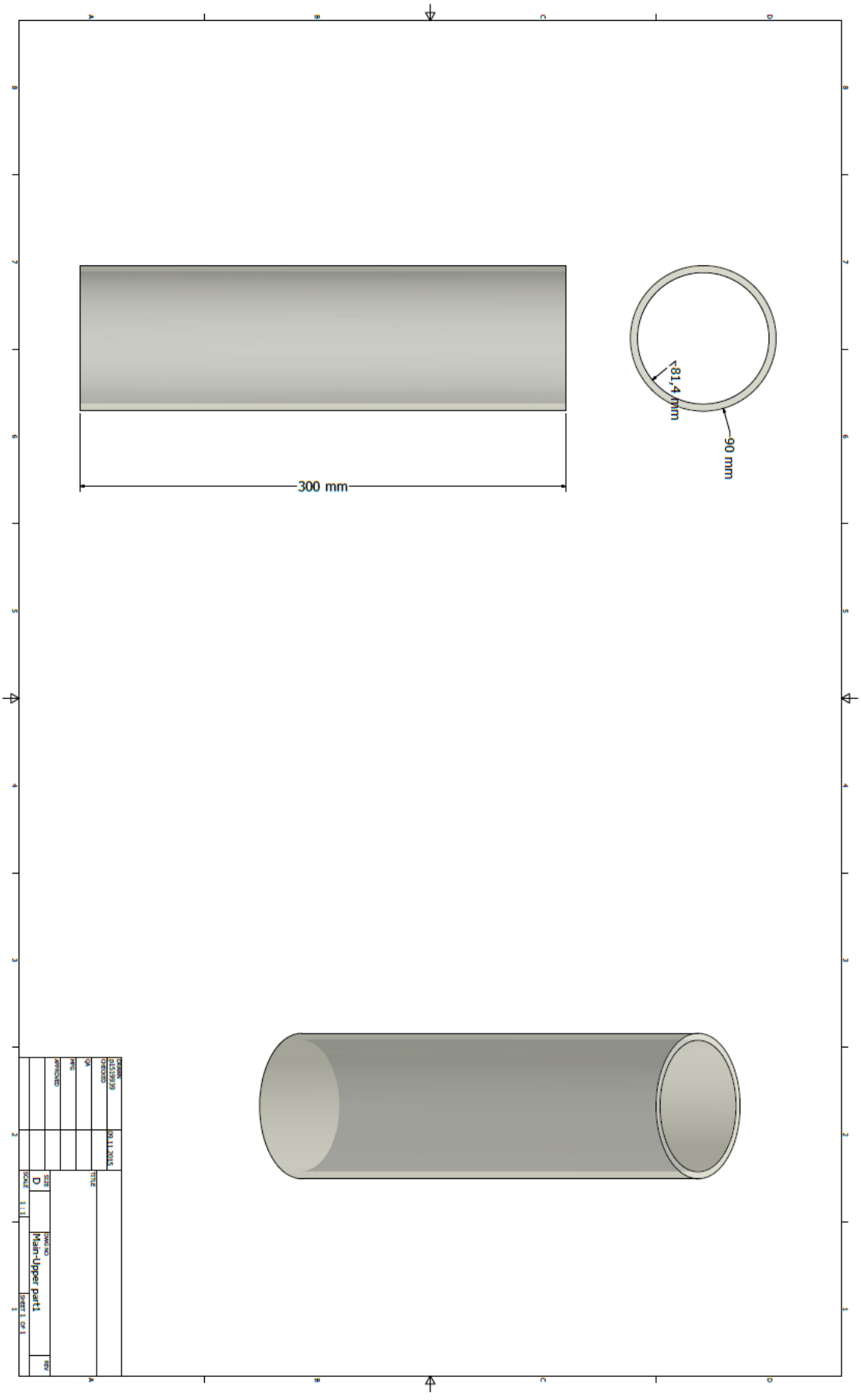

Appendix 3: Feed Port

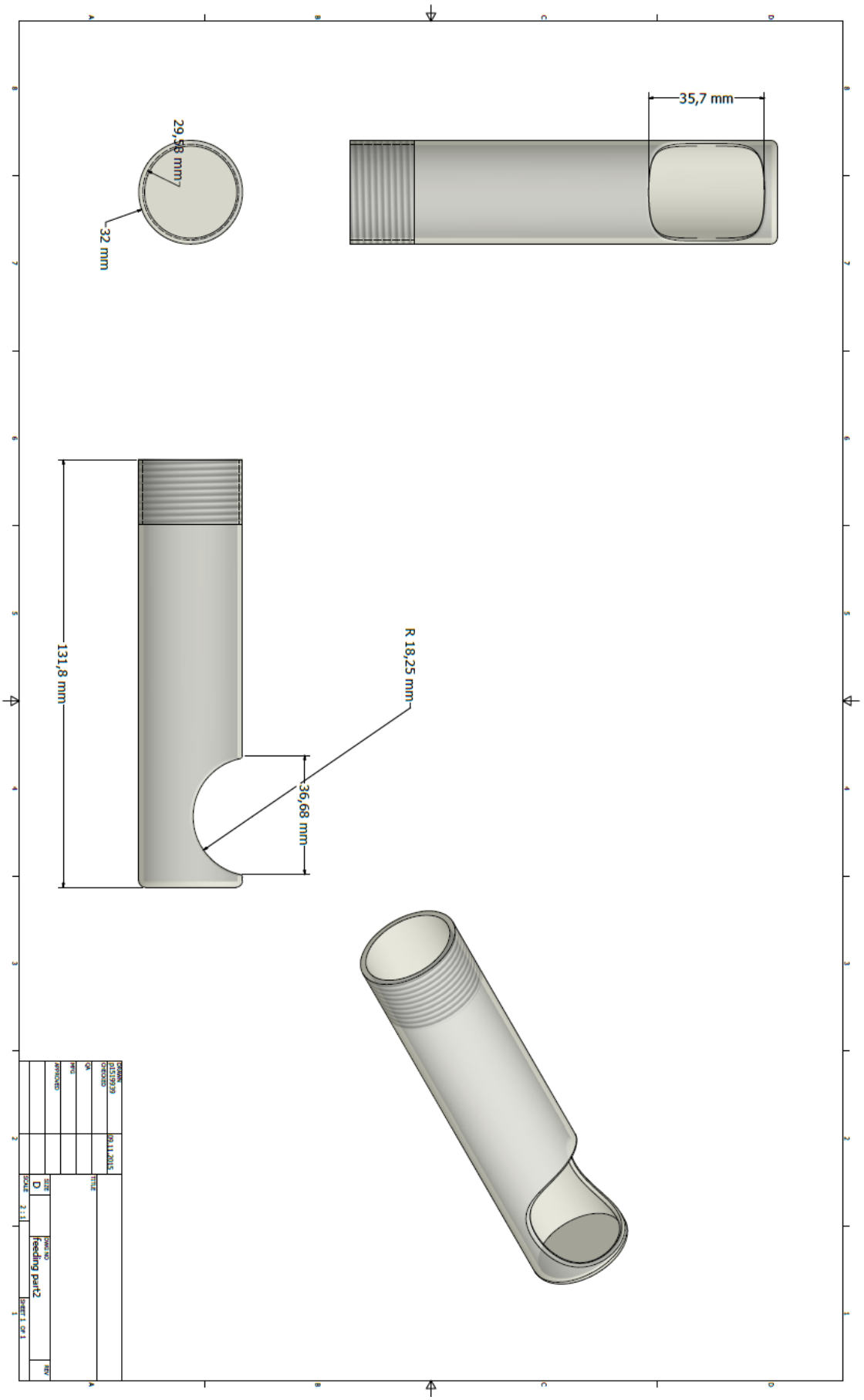

Appendix 4: Assembled Feed Port on the Body of Cell

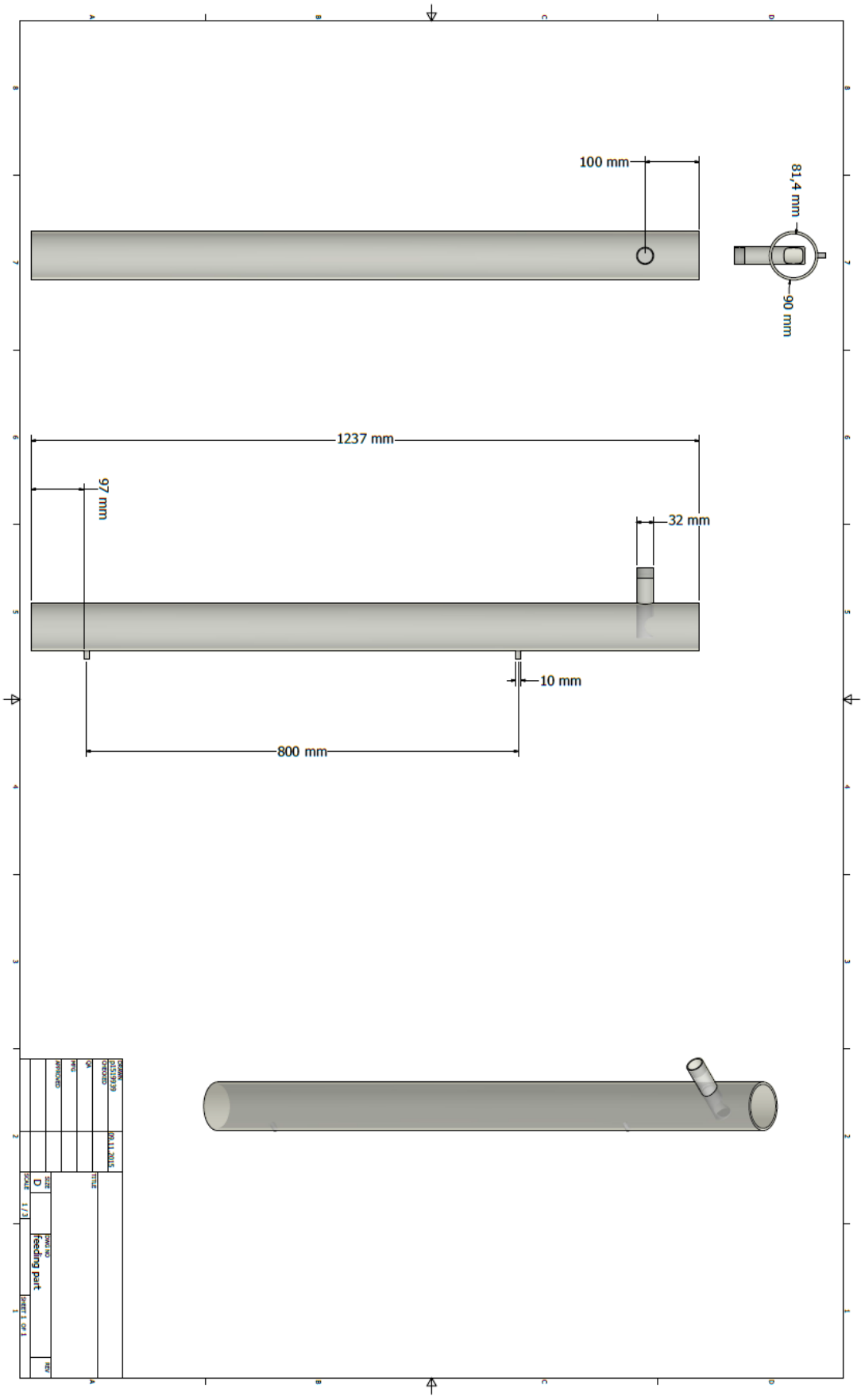

Appendix 5: Main Body Cell of Bubble Generator Holder

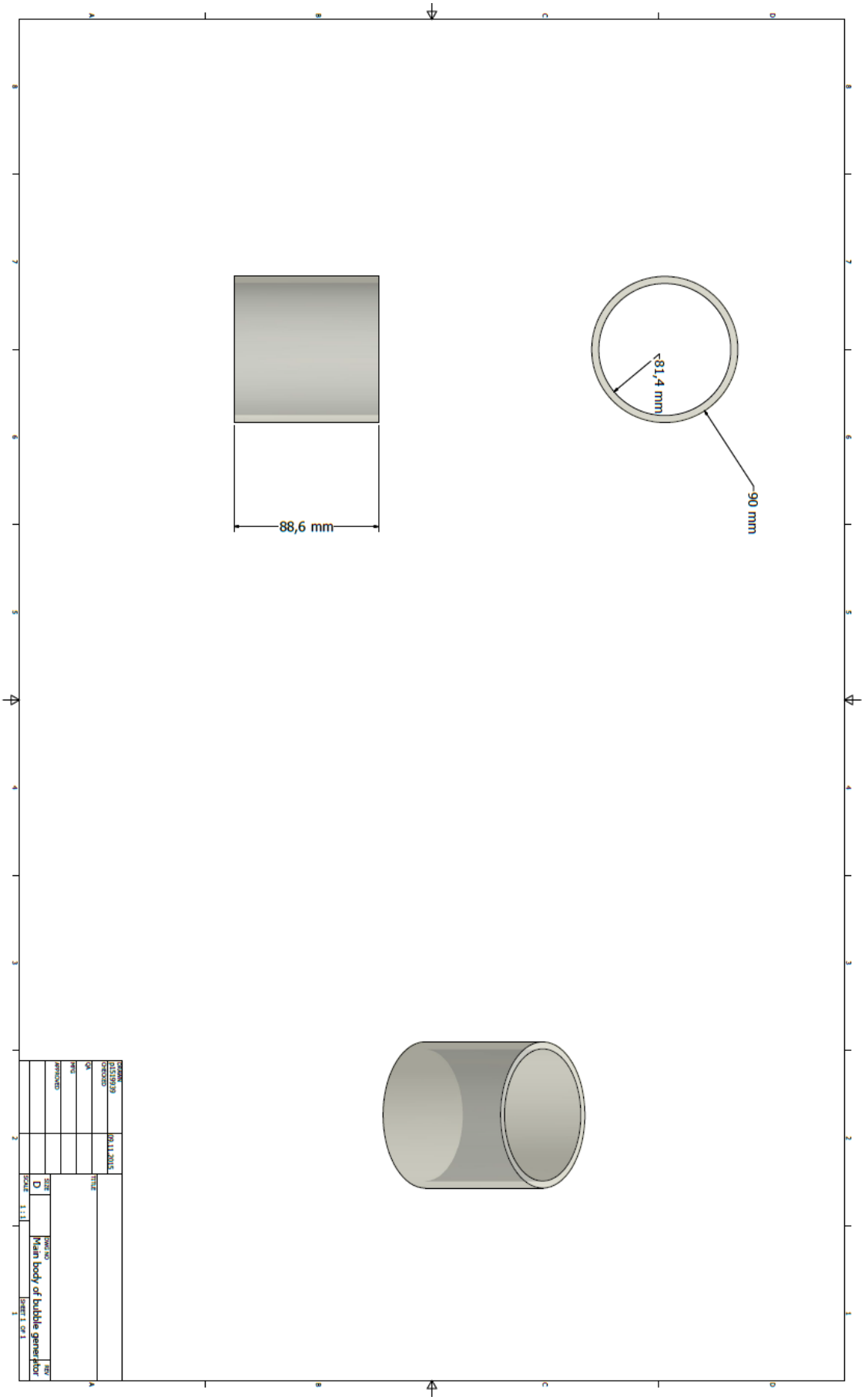

Appendix 6: Bottom Conical Part

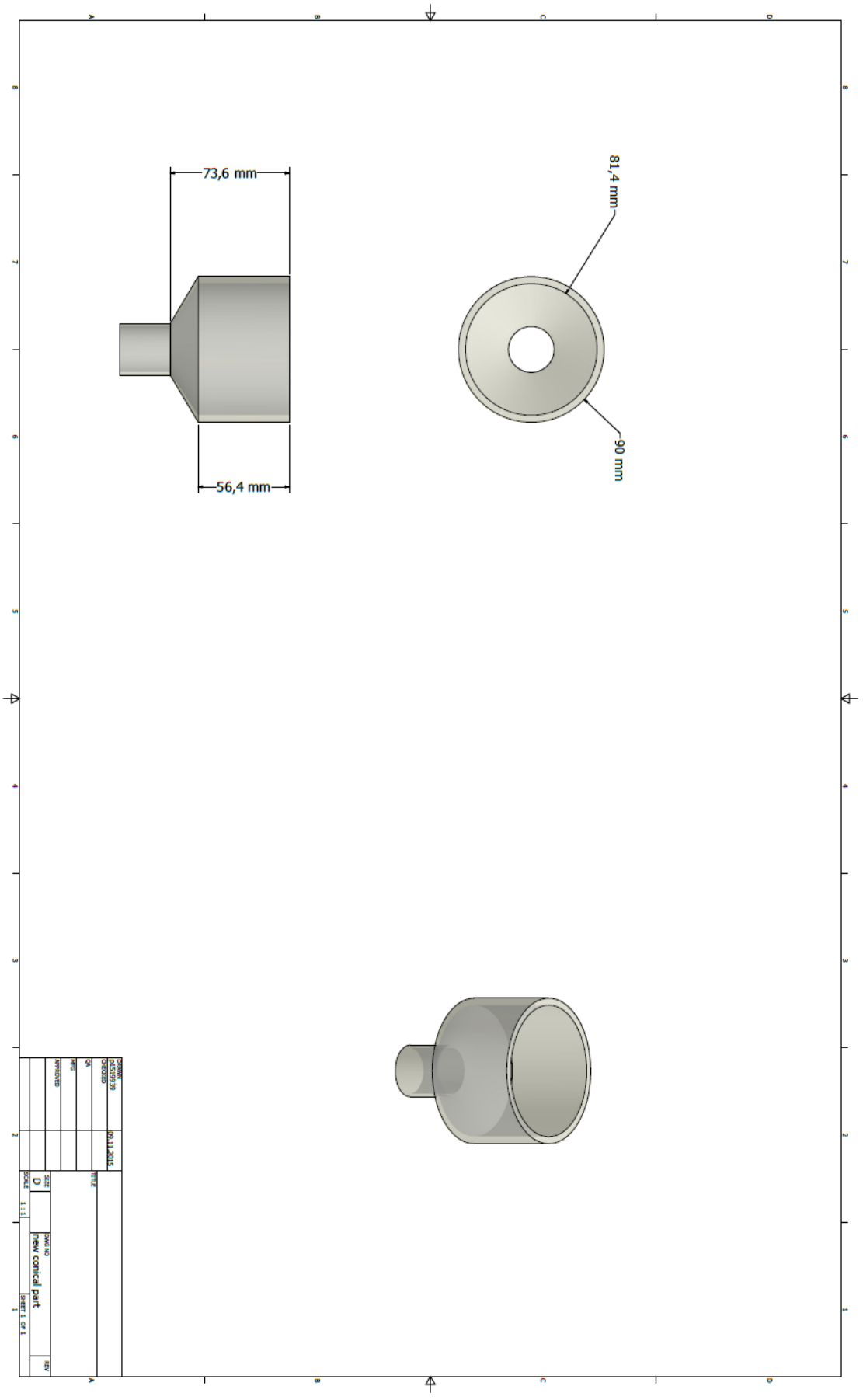

Appendix 7: Bubble Generator Holder

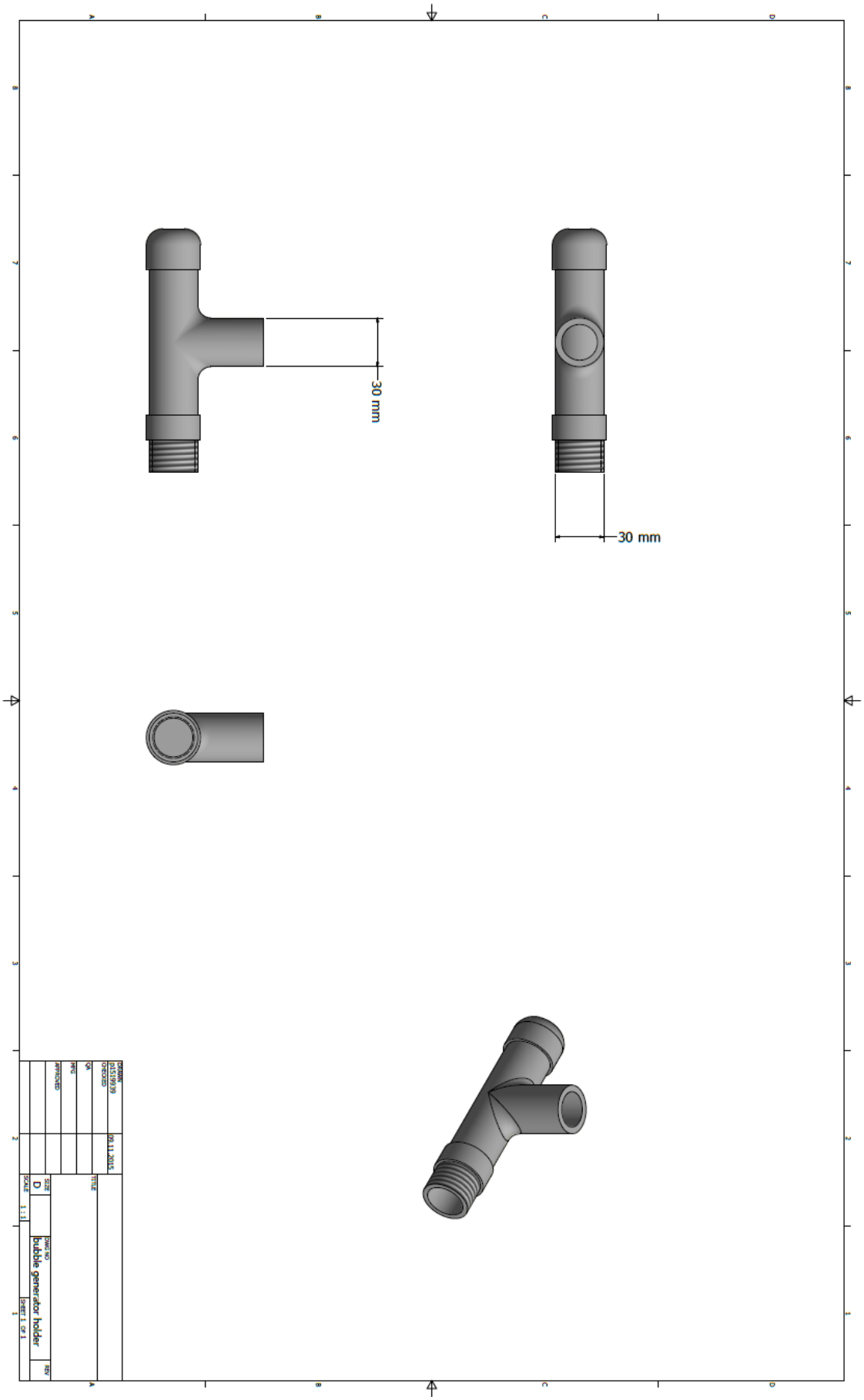

Appendix 8: Assembled Flotation Cell

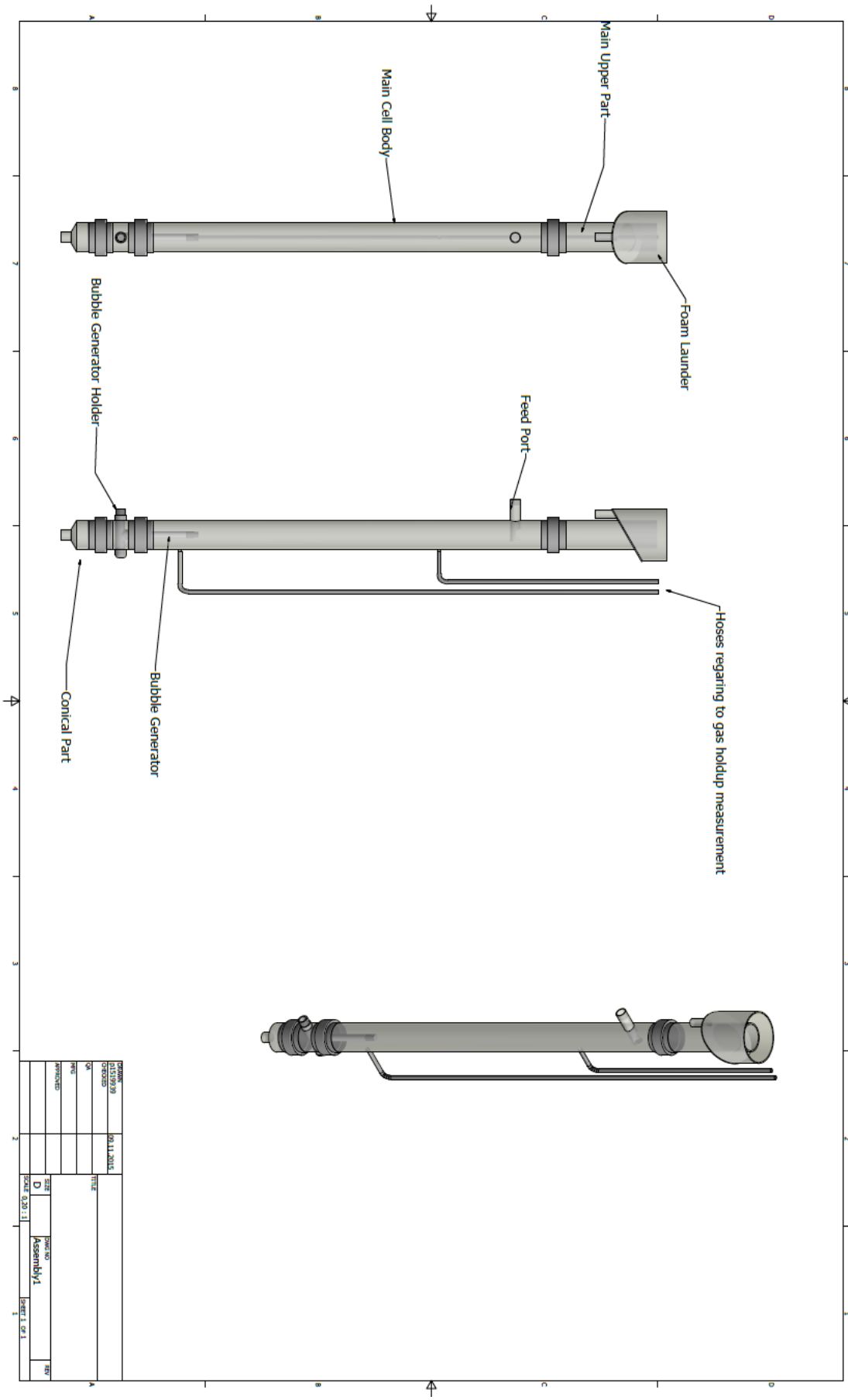

Appendix 9: Details of applied parts

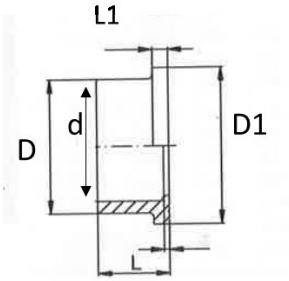

Part Name	Material	Code	d	D	L	L1
Flanged bushings	PVC-U	721 790 113	90 mm	108 mm	56 mm	11 mm

Part Name	Material	Code	d
Union nut	PVC-U	161 490 546	110 mm

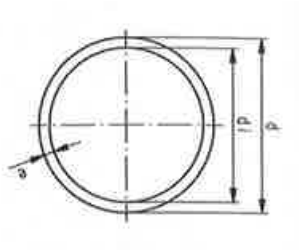

Part Name	Material	Code	d	e	Di
Pipe	PVC-U	192 017 088	90 mm	4,3 mm	81,4 mm